

1 **Geochemical controls on the partitioning and hydrological**  
2 **transport of metals in a non-acidic river system**

3  
4 **J. Thorslund<sup>1</sup>, J. Jarsjö<sup>1</sup>, T. Wällstedt<sup>2</sup>, C. M. Mörrth<sup>3</sup>, M. Yu. Lychagin<sup>4</sup> and S. R.**  
5 **Chalov<sup>4</sup>**

6 [1]{Department of Physical Geography and Quaternary Geology and the Bolin Centre for  
7 Climate Research, Stockholm University, SE- 106 91 Stockholm, Sweden}

8 [2]{Department of Applied Environmental Science, Stockholm University, Stockholm  
9 University, SE- 106 91 Stockholm, Sweden}

10 [3]{Department of Geological Sciences, Stockholm University, SE-106 91 Stockholm,  
11 Sweden}

12 [4]{Lomonosov Moscow State University, Faculty of Geography, 119991 Leninskie gory, 1,  
13 Moscow, Russia}

14  
15 Correspondence to: J. Thorslund (josefin.thorslund@natgeo.su.se)

Formatted: Numbering: Continuous, Different first page header

Formatted: Space After: 5.85 pt

## 18 Abstract

19 The speciation of metals, i.e., the chemical forms in which the metals occur, controls their  
20 mobility, bioavailability and toxicity. The overall objective of this study is to expand the  
21 knowledge of the spreading of metals in non-acidic river systems. This knowledge is currently  
22 much more limited than that of the behaviour of metals under acidic conditions (e.g., in acid  
23 mine drainage systems). We combine novel measurements of metal spreading under distinctly  
24 high-pH conditions (up to 9.6) along two rivers and in surface water ponds (in the Upper Lake  
25 Baikal Drainage Basin, Mongolia) with a geochemical modelling approach (Visual MINTEQ).  
26 ~~One of the~~The longer river ~~of the twos~~, the Tuul River, flows through a major gold mining site  
27 and was selected ~~as a focus reach for a main application example mass flow quantifications,~~  
28 ~~to investigate the impact of a large mining site on the transport of metals.~~ Total mass flows of  
29 several metals (Al, Cd, Fe, Mn, Pb and V) showed net increases across the gold mining site,  
30 with metals in suspension generally dominating the total export from the site. The model  
31 results ~~showed~~ indicated that a primary difference between non-acid and acid mine drainage  
32 geochemistry is that the prevailing high pH in the former causes the precipitation of  
33 ferrihydrite and gibbsite, which removes between 90 and 100 % of the Fe and Al from  
34 solution. This effect additionally influenced the behaviour of As, Pb and V, for which the  
35 solubilities were predicted to mainly be controlled by sorption onto ferrihydrite. The  
36 combined effects of such geochemical processes (precipitation and sorption) thus explain the  
37 high impact of suspended transport relative to total transport under non-acidic conditions.  
38 Furthermore, As showed dissolved concentrations above the health risk-based guideline  
39 values in several locations and thus is of main toxic concern in the Upper Lake Baikal  
40 Drainage Basin. Moreover, the present modelling showed that the solubility of Fe, Pb and Zn,  
41 in particular, can increase considerably, due to metal-organic complexation, as dissolved  
42 organic carbon (DOC) concentrations. In non-acidic systems, the seasonality of DOC  
43 concentrations can therefore have a major influence on the spreading and toxicity of these  
44 metals, as can DOC trends caused by land use change. The present results also suggest that the  
45 behaviour of Cr, Cu and Mo would be much better understood if a dependable adsorption

46 database for hydroxyapatite could be developed, since it seems likely that this mineral controls  
47 their solubilities.

48

49

50 *Keywords: metals, spreading, speciation, river system, alkaline, geochemical modelling,*  
51 *solubility, Lake Baikal*

52

53

## 54 **1 Introduction**

55 Metals can become exposed to the environment through natural processes, such as the  
56 weathering of soil and bedrock, and through anthropogenic processes, such as mining and  
57 other industrial activities and agriculture. Metals can enter aqueous systems through washout  
58 from surface soils, diffuse groundwater inflow, metal mobilisation from enriched sediments,  
59 leaching from agricultural areas and mine tailings, catastrophic tailings dam failure and the  
60 discharge of industrial and mining effluents (e.g., Hudson-Edwards 2003, Macklin et al.,  
61 2006, Mighanetara et al., 2009 and Inam et al., 2011). Material mobilisation via bank and bed  
62 erosion under conditions of geomorphic adjustment can dominate pollutant transport under  
63 certain conditions (Lewin and Macklin 1987 and Chalov et al., 2014). Once metals are  
64 released into aquatic systems, they persist because of their non-degradable nature. Metals held  
65 in alluvial stores may therefore continue to pose a threat to ecosystems long after their initial  
66 release, and alluvial sediments may constitute the greatest source of catchment heavy metal  
67 pollution (Alexeevsky et al., 2013).

68 Mounting evidence in recent decades has shown that the speciation of metals (i.e., the  
69 chemical forms in which they occur) controls their mobility, bioavailability and toxicity (e.g.,  
70 Tessier and Campbell 1979, Tack and Verloo, 1995, Tipping, 1998, Fytianos 2001 and  
71 Landner 2005). The dissolved form, especially the dissolved inorganic fraction, is considered  
72 to be the most toxic form of the majority of metals (e.g., Chapman et al., 1992, Gundersen and  
73 Steinnes, 2001 and Nystrand et al., 2012) because it can be readily taken up by organisms and  
74 biota (e.g., Törnqvist et al., 2011 and Raguz et al., 2013), in contrast to many suspended  
75 forms. Many chemical factors and parameters must be accounted for in determining the  
76 speciation of metals, such as pH, redox conditions, the oxidation state of the metal and the  
77 available surfaces for adsorption (e.g., Palleiro et al., 2013). An advantage of equilibrium  
78 speciation models is their ability to predict predominant forms of metals and evaluate the  
79 mechanisms controlling speciation, such as sorption and precipitation reactions (Lund et al.,  
80 2008). Frequently used speciation models include WHAM (Tipping 1994), PHREEQC  
81 (Parkhurst and Appelo, 1999) and Visual MINTEQ (Gustafsson 2009), which are used in both

82 groundwater and surface water applications (e.g., Tipping and Lawlor et al., 1998, Butler et  
83 al., 2004, Gustafsson et al., 2009, Korfali and Davies 2004, Wällstedt et al., 2010 and  
84 Nystrand et al., 2012). These models have the ability to simulate surface adsorption reactions  
85 and the complexation of metals with organic matter, which are central to metal transport and  
86 partitioning between the water and sediment phase (e.g., Butler et al., 2008).

87 Although there are many studies on speciation modelling of metals in aqueous systems (e.g.,  
88 Eary 1999, Butler et al., 2004, Balistrieri et al., 2007, Gustafsson et al., 2009 and Nystrand et  
89 al., 2012), the majority of these studies have focused on metal behaviour under acidic or near-  
90 neutral conditions rather than under high-pH conditions. Some exceptions include a study by  
91 Sjöstedt et al. (2009), who measured and modelled the speciation of Al, As and Mo in  
92 Swedish lakes that had been limed to near-neutral pH, and a study by Moldovan and Hendry  
93 (2005), who modelled the speciation of As, leaching from uranium mining, up to a pH of 11.

94 However, speciation studies focusing on large-scale spreading of multiple metals across scale  
95 in non-acidic hydrological systems are rare (Pandey et al., 2014 and Sungur et al., 2014),  
96 although a lot of research many studies have highlighted pollution problems of metals in these  
97 environments (see, e.g., Tarras-Wahlberg et al. 2000, Sjöblom et al., 2004, Grosbois et al.,  
98 2009 and Zak et al., 2009); often Non-acidic systems often showing high metal  
99 concentrations in particles but low concentrations in the dissolved form, thereby indicating  
100 that the geochemical controls and dominating processes might differ from well-studied acidic  
101 pollution sources water systems.

102 Furthermore, understanding geochemical controls in combination with the physical transport  
103 of metals could greatly enhance predictions of metal transport and fate (Foster and  
104 Charlesworth 1996, Destouni et al., 2010, Persson et al., 2011). For example, geochemical  
105 processes (e.g., adsorption) influence whether certain physical processes (e.g., suspended  
106 sediment transport; Chalov et al., 2012) will be important in the overall transport of metals.  
107 However, relatively few studies have addressed these combined effects of physical and  
108 chemical controls on metals in aqueous systems (e.g., Caruso et al., 2008 and Malmström et

109 al., 2008, Butler et al., 2009); ~~to our best knowledge, and none of them considered, to our~~  
110 ~~knowledge, in~~ non-acidic streams.

111 The overall objective of the present study is to extend the knowledge on the spreading of  
112 metals in non-acidic river systems. We combine novel site-specific measurements with a  
113 geochemical modelling approach (Visual MINTEQ), specifically aiming to (i) evaluate the  
114 performance of this modelling approach by comparing observations and model predictions,  
115 (ii) identify dominant solids and predict the capacity of these solids to sorb and/or co-  
116 precipitate other metals that are transported in suspension and (iii) identify the dominant  
117 controls keeping metals in solution, such as soluble complexation.

118 As application examples, we consider the distinctly high-pH conditions of the Tuul and  
119 Sharyngol Rivers, ~~two rivers which are~~ both influenced by mining activities and located in the  
120 upstream Lake Baikal basin, Mongolia (Pietron 2012, Thorslund et al., 2012, Chalov et al.,  
121 2012 and Chalov et al., 2014). We also ~~include~~ ~~consider~~ small surface water ponds ~~within~~  
122 ~~from~~ the largest mining site in Mongolia, ~~comprising a widespread source zone; namely the~~  
123 Zaamar Goldfield which is located along the Tuul River ~~and comprises a widespread source~~  
124 ~~zone~~. The ~~Tuul River~~ ~~latter~~ connects to the Orkhon-Selenga River system and is a highly  
125 polluted river in the upstream Mongolian part of the transboundary Russian-Mongolian Lake  
126 Baikal drainage basin. The many mining companies within the Zaamar Goldfield, as well as  
127 illegal mining, are considered to have a serious impact on the water quality within the river  
128 basin (Altansukh and Davaa 2011, Chalov et al., 2012 and Thorslund et al., 2012) and may  
129 have an impact on the downstream Selenga River and Lake Baikal. Although total (suspended  
130 and dissolved) concentrations and estimated mass flows of several metals within this system  
131 were high, the dissolved fractions were generally low (Thorslund et al., 2012). In the  
132 downstream regions of the Lake Baikal drainage basin, however, increasing metal pollution of  
133 both sediments and biota has been reported (e.g., Rudneva et al., 2005 and Khazheeva et al.,  
134 2006). Investigating controls on metal partitioning between the sediment and water phase is  
135 thus of particular importance for this system because metals originating from the Zaamar

136 Goldfield may be transported all the way to the vicinity of Lake Baikal, which hosts a unique  
137 ecosystem and represents a major water resource.

## 138 **2 Site description**

139 The Tuul River and the Sharyngol River are both located in the upstream Lake Baikal basin,  
140 Mongolia (see Fig. 1 and Table 1 for sampling locations and coordinates). The Sharyngol river  
141 basin is about half the size of the Tuul River basin (MCA 2011). Both rivers are tributary  
142 ivers to the Orkhon-Selenga river system, with the transboundary Selenga River being by far  
143 the largest river draining into Lake Baikal (Lee et al., 2006), discharging approximately 30  
144 km<sup>3</sup> of water and 3.5 million tons of sediments annually into the lake. Before the Selenga  
145 River flows into Lake Baikal, it flows through the Selenga delta, covering an area of  
146 approximately 1200 km<sup>2</sup> (USGS 2011).

147 The mining areas of the Zaamar Goldfield are located in the Tuul River valley, between  
148 latitude 48°17'50" N and longitude 104°24'65" E (Fig. 1) (AATA 2008), approximately 600  
149 km upstream of the Lake Baikal inlet (AATA 2008). The Tuul River is a tributary of the  
150 Selenga River, a transboundary river between Mongolia and Russia and by far the largest river  
151 draining into Lake Baikal (Lee et al., 2006), discharging approximately 30 km<sup>3</sup> of water and  
152 3.5 million tons of sediments annually into the lake. Before the Selenga River flows into Lake  
153 Baikal, it flows through the Selenga delta, covering an area of approximately 1200 km<sup>2</sup> (USGS  
154 2011).

155 The annual average discharge of the Tuul River is 27 m<sup>3</sup>/s (1945-2007), but maximum  
156 discharges in the summer period can reach approximately 80 m<sup>3</sup>/s, whereas lower discharges  
157 occur throughout the coldest months of the year (November-March). Below the confluence of  
158 the Tuul River with the Orkhon River, discharges increase on average by an order of  
159 magnitude, and in the downstream Selenga River, the annual average discharge reaches just  
160 over 1000 m<sup>3</sup>/s (GEMStat 2011, MCA 2011). The Sharyngol annual average discharge is  
161 much lower than for the Tuul River, with long term average (1977-2007) of only 1.7 m<sup>3</sup>/s  
162 (MCA 2011). The average annual precipitation in the region is between 200 and 250 mm. The

163 climate of the region is semi-arid with warm and dry summers (average temperatures of 20  
164 °C), although intense rainfall does occur, and cold winters (average temperatures of -20 °C)  
165 (AATA 2008).

166 The geology of the area includes sedimentary, igneous, and metamorphic rock formations,  
167 such as sedimentary sandstones and siltstones, igneous gabbros, and metamorphic schists. The  
168 region also naturally contains calcium bicarbonates to a large degree (Altansukh and Davaa  
169 2011), and there are strong interactions between surface waters and groundwater due to  
170 extensive areas of alluvial unconfined aquifers in the river valleys (Zandaryaa et al. 2008).

171 This condition impacts both the Tuul and Sharyngol River quality and quantity because the  
172 river is fed by groundwater inflows with high water-rock interactions. These interactions  
173 cause the pH values throughout the Zaamar Goldfield region to be very high (Lee et al., 2006  
174 and Zandaryaa et al., 2008).

175 Both of these rivers are also impacted by mining activities, with placer gold mining in the  
176 Tuul river basin and open pit coal mining in Sharyngol (MCA 2011). The mining areas of the  
177 Zaamar Goldfield are located in the Tuul River valley, between latitude 48°17'50" N and  
178 longitude 104°24'65" E (Fig. 1) (AATA 2008), approximately 600 km upstream of the Lake  
179 Baikal inlet (AATA 2008). Zaamar Goldfield is the largest gold mining site within the Tuul  
180 basin and the extensive source zone contains both alluvial and hard rock mining that stretches  
181 for approximately 45 km along the floodplain of the Tuul River (Lee et al., 2006). The  
182 abundant mining activities over a widespread area and the lack of control of tailing and  
183 leakage from settling ponds contribute to both diffuse and direct pollution of soil, groundwater  
184 and surface water (Zandaryaa et al., 2008). High levels of metals have been measured in the  
185 Tuul River (Lee et al., 2006 and AATA 2008), and previous mass balance quantifications  
186 have shown a net increase in metal loading over the mining zone, especially of metals in  
187 suspension (Thorslund et al., 2012).



## 188 3 Methods of data collection and analysis

### 189 3.1 Field methods and sample collection

190 Water samples were collected during two field campaigns, one in June 2012 and one in  
191 September 2013. In the first year, ~~only a focus reach of the Tuul River;~~ at five locations  
192 around the Zaamar Goldfield at the Tuul River (T5, T5a, T5b, T6, T6a), were sampled. ~~This~~  
193 ~~reach~~ These locations were ~~was~~ chosen due to previous quantifications in this region since  
194 independent quantifications exist for them, for instance showing that and the identification of  
195 Zaamar is as an important source zone with high transport of metals. ~~During~~ In the second  
196 year, sampling of the five locations around Zaamar Goldfield ~~the Tuul focus reach sampling~~  
197 ~~was repeated~~ but. In addition, sampling of 12 more new locations with high pH in the region  
198 was performed; five additional ones from the Tuul River (T2, T3, T4, T6b, T7) four from  
199 Sharyngol River (S1, S2, S3, S5) and three from ponds at the Zaamar site (P1, P3, P4). The  
200 pond water consist of waste water from washing out the gold from metal enriched sediments.  
201 Information on the sampling locations, including coordinates, is shown in Table 1 and Fig. 1.

202 Relatively low water discharges were observed during the June 2012 campaign ( $Q = 13\text{--}15$   
203  $\text{m}^3/\text{s}$ ), whereas substantial flooding with floodplain inundation was documented during the  
204 September 2013 field campaign ( $Q = 45\text{--}52 \text{m}^3/\text{s}$ ). The hydrometeorological conditions also  
205 varied between the seasons, e.g., relatively dry weather during the 2013 campaign and  
206 abundant rainfall in the 2012 campaign.

207 The sampling procedure included grab sampling of water in plastic polypropylene bottles (500  
208 ml) just below the surface of the sampled water. All sampling bottles were rinsed with the  
209 selected water before collecting the sample for analysis. The bottled water was then  
210 transferred into two high-density polypropylene test tubes (10 ml): one unfiltered sample and  
211 one filtered sample (filtered through a sterile  $0.20 \mu\text{m}$  pore membrane filter, prewashed with  
212 sample water). In the 2013 campaign, three replicates of both filtered and unfiltered samples  
213 were collected. All test tubes were sterile and rinsed thoroughly with the sampled water before  
214 collecting the sample for analysis. The samples were acidified (1 %) with concentrated  $\text{HNO}_3$

215 (65 %) to preserve them for analysis and prevent the precipitation of metals. In the following  
216 text, unfiltered metal concentrations are referred to as total concentrations, while the filtered  
217 concentrations are referred to as dissolved fraction, using a similar nomenclature as for  
218 TOC/DOC.

219 The temperature and pH were measured in situ, directly in the rivers and ponds, using a  
220 Hannah Instrument (HannahNorden, Sweden, Kungsbacka) HI 9828 meter (2012) and an HI  
221 98108 (2013). The meters were calibrated with pH 7 and pH 10 solutions before each  
222 measurement campaign and then recalibrated during the campaigns. For the 2012 campaign,  
223 the alkalinity was measured at Moscow State University using the standard titration method,  
224 whereas for the 2013 campaign, alkalinity was measured using a Total Alkalinity test kit (HI  
225 38014) directly in field.

226 Additionally, in the 2013 campaign, samples for total and dissolved organic carbon  
227 (TOC/DOC) were collected from all locations. Samples were collected in 30 ml high-density  
228 polypropylene test tubes (three replicates) and samples for DOC analysis were filtered with  
229 0.22 µm pore membrane filters. All samples were acidified (1 %) with concentrated acid  
230 HNO<sub>3</sub> (65 %) and wrapped in aluminum foil to prevent light from penetrating the samples.  
231 These procedures were all performed directly in the field. In 2013, samples were also  
232 collected for anion (F<sup>-</sup>, Cl<sup>-</sup>, NO<sub>3</sub><sup>-</sup>, SO<sub>4</sub><sup>2-</sup>, Br<sup>-</sup>) analysis in 10 ml high-density polypropylene test  
233 tubes (three replicates), without further preparations.

### 234 **3.2 Analytical methods**

235 All samples discussed in the present paper were analysed at Stockholm University. The metal  
236 concentrations were determined by inductive coupled plasma optical emission spectrometry  
237 (ICPOES) with a Thermo iCAP 6500 Duo analyser to determine the contents of the following  
238 metals: Al, As, B, Ba, Ca, Cd, Co, Cr, Cu, Fe, K, Mg, Mn, Mo, Na, Ni, P, Pb, S, Si, Sn, Sr, Ti,  
239 V and Zn. The analysis of samples followed standard procedures using a micro concentric  
240 nebuliser and, in some cases, an ultra sonic nebuliser, CETAC USN U5000AT+, to obtain  
241 better detection limits.

242 TOC/DOC concentrations were determined using an NPOC (non-purgeable organic carbon)  
243 measurement in a Shimadzu TOC-L CPH analyser. The major anion analysis was performed  
244 by liquid chromatography using the IC20 Dionex following standard Swedish procedures  
245 (EN-ISO 10304-1:2009).

### 246 3.3 Discharge measurements and mass flow estimates

247 Discharge was measured at the five sampling locations ~~around the Zaamar Goldfield along the~~  
248 ~~focus reach of~~ at the Tuul River (T5, T5a, T5b, T6, T6a), both in 2012 and 2013 and at the  
249 same places and times as the collection of water samples for chemical analysis. The  
250 measurements were made by wading, by boat or from bridges (depending on the depth of each  
251 river section). Velocities were measured with a hydrometric propeller (ISP-1) at 0.6 m depth  
252 (from the surface) at each width increment. When the depth exceeded 1.5 meters, an Acoustic  
253 Doppler Profiler (ADP) was used, which measures water level and velocity in horizontal  
254 profiles across a channel.

255 The discharge of each cross-section was calculated according to Eqs. (1) and (2):

256

$$257 \quad Q = \sum_1^n V_n \cdot A_n \cdot k \quad (1)$$

258

259 where  $V_n$  is the velocity of each width increment and  $A_n$  is the area of each rectangular  
260 subsection, using the Trapezoidal rule; and

261

$$262 \quad A_n = \frac{d_n + d_{n-1}}{2} \cdot (b_n - b_{n-1}) \quad (2)$$

263 The coefficient  $k$  in Eq. (1) is used when the expression is applied to non-steep banks; here,  $k$   
264 is equal to 0.7 (Bykov and Vasil'ev 1972). In Eq. (2),  $d$  is the depth of each subsection and  $b$  is  
265 the distance from the bank.

266 The discharges,  $Q$ , were multiplied with the concentrations,  $C$ , according to Eq. (3) to yield  
267 estimates of the dissolved and total metal mass flows,  $Mf$ , for the five cross-sections along the  
268 Tuul River.

$$269 \quad Mf = C \cdot Q \quad (3)$$

270 The simultaneous measurements of pollutant concentrations and discharges were made to  
271 obtain snapshot values of loads along the river reach and across the Zaamar mining site.

### 272 **3.4 Modelling approach**

273 Eleven metals were selected from the analytical results dataset for further interpretation and  
274 modelling purposes: Al, As, Cd, Cr, Cu, Fe, Mn, Mo, Pb, V and Zn. These metals were  
275 selected because they are often found at mining sites (e.g., Hudson-Edwards 2003) and  
276 because of their potential toxicity to humans and biota. Mercury (Hg) is a metal that is often  
277 associated with mining activities but was excluded here because it requires different analytical  
278 procedures from those performed here, i.e., the fluorescence method. Furthermore, previously  
279 reported measurements have repeatedly shown that Hg concentrations have been low and in  
280 many cases below detection limits in recent years (2006-2011) (Thorslund et al., 2012).

281 The geochemical equilibrium model Visual MINTEQ vers. 3.0 (Gustafsson 2011) was used to  
282 model the speciation of the eleven selected metals. This model calculates the chemical  
283 composition of various inorganic ions in aqueous systems at a single point (e.g., a water  
284 sample) under the assumption of a chemical equilibrium state. For inorganic complexes, the  
285 thermodynamic default database in Visual MINTEQ was used, which is mostly based on the  
286 NIST compilation (Smith et al., 2003).

287 Complexation of the metals with dissolved organic matter was modelled using the  
288 'Stockholm humic model' (SHM) (Gustafsson, 2001) with its default database. This model  
289 uses a discrete-site approach to represent the metal humic complexation, similar to the model  
290 described by Tipping (1994). The default ratio of 1.65 between active DOM (i.e., the part of  
291 the organics that binds to the metals) and DOC was assumed to be representative based on a

292 study by Sjöstedt et al. (2010) and thus not changed. All of the DOM was assumed to be fulvic  
293 acid based on previous studies (e.g., Khai et al., 2008, Sjöstedt et al., 2010, Wällstedt et al.,  
294 2010 and Gustafsson et al., 2014).

295 The input variables for each sampling point were the following: total concentrations of all  
296 elements analysed (see Table 2 for the selected oxidation states), major anion concentrations,  
297 pH, alkalinity ( $\text{HCO}_3^-$ ), temperature, pe (redox potential) and DOC (see Table 4 for input  
298 values). Previous studies (e.g., Nystrand et al., 2012) have shown that modelling results are  
299 more accurate if they are based on concentrations of a relatively large number of elements in  
300 the input data because this provides a better representation of the chemistry in the water  
301 sample (ionic strength and complex binding is then better represented) and thus decreases  
302 uncertainties in model calculations. The concentration data of all elements determined in the  
303 ICP-OES analysis were therefore used as input variables (see Sect. 3.2). However, in the  
304 subsequent sections, the model outputs for the eleven selected metals are presented and  
305 furthered discussed.

306 The DOC and major anions were not measured during the field campaign in 2012. Thus, for  
307 the modelling of the 2012 data, the DOC values from the 2013 campaign were used. In  
308 addition ~~to this~~, 50 % higher DOC values than the measured ones were ~~simulated used for in~~  
309 scenario simulations of all locations to investigate the sensitivity to changing DOC  
310 concentrations, as well as ~~a test simulation one some locations~~ simulations where DOC  
311 concentrations were ~~excluded~~ assumed to equal zero. Because sulphate ( $\text{SO}_4^{2-}$ ) and chloride  
312 ( $\text{Cl}^-$ ) concentrations were not measured in the 2012 campaign, they had to be approximated.  
313 Sulphate concentrations were assumed to be equal to half of the measured sulphur (S)  
314 concentrations, and chloride concentrations were set to equal the measured sodium (Na)  
315 concentrations.

316 The pe was estimated according to Eq. (4) for both years, which is assumed to be  
317 representative of well-oxygenated waters (Stumm and Morgan 1996).

318 
$$pe = 20.77 + \frac{1}{4} \log P_{O_2} - pH \quad (4)$$

319

320 where  $P_{O_2}$  is assumed to equal 0.2 atm (i.e., the  $O_2$  content in the atmosphere is 20.95 %),  
321 similar to the value used by Wällstedt et al. (2010). The estimated values should be  
322 considered as maximum values, since the redox reaction for  $O_2$  is slow and the pe-values of  
323 natural waters are in reality often lower than the theoretical values (Langmuir, 1997).

324

325 The solids that were allowed to precipitate when their respective solubility constants were  
326 exceeded are shown in Table 3. These solids were chosen based on (i) knowledge of common  
327 solids for the present geological conditions of the study site and (ii) model outputs of  
328 ‘saturation indices’, indicating which minerals could precipitate based on site-specific data  
329 and thermodynamic calculations. For ferrihydrite,  $Fe_2O_3 \cdot 1.8H_2O$ , the solubility constant  
330 selected was one for ‘aged’ ferrihydrite with  $\log *K_s = 2.69$  at 25 °C (Smith et al., 2003).  
331 This is in the lower range of constants reported for “amorphous iron hydroxide”, “hydrous  
332 ferric oxide”, etc. ( $\log *K_s = 2.5-5$ ; Tipping et al., 2002). This model approach has  
333 previously been shown to produce reliable modelling results for Fe that agree well with  
334 analytical results (Sjöstedt et al., 2013). Ferrihydrite is an iron mineral that is frequently used  
335 as a solid for adsorption in Visual MINTEQ, and the adsorption database for this solid is thus  
336 extensive. Ferrihydrite is well known for its metal retention capacity due to large specific  
337 surface area and has been shown to correlate well with measured data (e.g., Sjöstedt et al.,  
338 2010, Nystrand et al., 2012 and Tiberg et al., 2013).

339 For Gibbsite (C), the solubility constant with  $\log *K_s = 7.74$  at 25 °C (Smith et al., 2003) was  
340 selected. -The published data on the solubility of gibbsite vary and are mainly a function of  
341 pH, sulphate, fluoride and DOC concentrations. The main difficulty lies in that it is difficult to  
342 separate amorphous  $Al(OH)_3$  from gibbsite in natural systems. Because of this difficulty, the  
343 solubility of Al is restricted, and its database in Visual MINTEQ is more limited than for  
344 ferrihydrite.

345 For modelling of adsorption, ferrihydrite and gibbsite were chosen as possible solid phases,  
346 due to their high measured particulate concentrations and their sorption capacities. The  
347 adsorption was estimated using the diffuse layer model (DLM) using the default database in  
348 Visual Minteq based on Dzombak and Morel (1990) and Karamalidis and Dzombak (2010)  
349 respectively. The only exception was vanadate adsorption to ferrihydrite where the adsorption  
350 constants were changed based on Wällstedt et al (2010).

351 To test the impact of varying conditions on model predictions, both pH and pe were changed  
352 from site specific values for each sample location. Model simulations were conducted for two  
353 different acidic pH conditions: pH 3.5 and pH 6 and pe was lowered by 50 %.

## 354 **4 Results**

### 355 **4.1 Tuul River water chemistry**

356 The representative geochemical parameter values, used for the model input, of the sampling  
357 locations along the Tuul River (T2, T3, T4, T5, T5a, T5b, T6, T6a, T6b, T7), the Sherengol  
358 River (S1, S2, S3, S5) and ponds (P1, P3, P4) are shown in Table 4. The pH indicates neutral  
359 to alkaline conditions in all cases, with average values of 8.3 (Tuul), 8.2 (Sherengol) and 8.7  
360 (ponds). ~~The DOC concentrations are similar for all sampled locations, however -are within~~  
361 ~~the same range~~ with average values being slightly higher for ~~the~~ Sherengol River (10.7) than  
362 for the Tuul River (10.4 mg/l) and the ponds (9.6 mg/l). The TOC concentrations were on  
363 average only a few per cent higher than the DOC concentrations; hence, the DOM dominates  
364 the total organic matter composition. The estimated alkalinity values are very high, especially  
365 from the field measurements in 2013.

366 Dissolved and total riverine concentrations ~~for for the focus reach of the~~ reach of Tuul River  
367 that was sampled both years (T5, T5a, T5b, T6, T6a), representing the proximity of Zaamar  
368 Goldfield ~~the mining site~~ (upstream, at site, downstream), are shown in Fig. 2 a to k. The  
369 results show that concentration levels are generally in the same order of magnitude during  
370 both snapshot measurements (2012 and 2013), with the exception of total concentrations of

371 Al, Cd and Mn, which are up to one order of magnitude greater in the 2012 campaign. The  
372 differences between particulate and dissolved concentrations are greatest for Al, Fe and Mn,  
373 with particulate concentrations being on average 178, 35 and 25 times greater, respectively,  
374 than dissolved concentrations in the 2012 campaign and 42, 18 and 5 times greater,  
375 respectively, in the 2013 campaign. As, Cd, Cr, Cu and Mo have dissolved concentrations in  
376 the same order of magnitude as their total concentrations. V and Zn show varying behaviour,  
377 both having higher dissolved and particulate concentrations depending on the sampling point.

378 Overall, the total concentrations show a net increase over the site, with higher values for the  
379 most downstream point (T6a) compared to the upstream points (T5, T5a), with the exception  
380 of Zn and Mo. Several metals (Al, As, Fe and Mn) show total (unfiltered) concentrations that  
381 exceed WHO and Mongolian health risk-based guideline values (Appendix A). Additionally,  
382 As exhibits dissolved (filtered) concentrations exceeding these health risk-based guideline  
383 values. Nevertheless, a comparison with data on monthly average concentrations for the Tuul  
384 River during summer or autumn months of 2005, 2006 and 2008 indicate that concentrations  
385 can be higher in this system (Thorslund et al., 2012) than observed during the here considered  
386 2012 and 2013 campaigns.

## 387 **4.2 Riverine mass flows**

388 The dissolved and total (dissolved + suspended) mass flows around Zaamar Goldfield at the  
389 Tuul River ~~focus reach~~ (T5, T5a, T5b, T6, T6a) from both campaigns are shown in Fig. 3 a to  
390 k (note the different scales on the y-axis). The first location (T5) is not included in the 2013  
391 campaign due to missing discharge data. Taken together, the majority of metals from both  
392 campaign years show net increasing total mass flows across the Zaamar Goldfield, with values  
393 being higher at the farthest downstream point (T6a) than the farthest upstream (T5, T5a)  
394 points. Due to the previously noted large dissolved and total concentration differences, the  
395 differences between dissolved and total mass flows are generally high, with total mass flows  
396 up to two orders of magnitude higher than dissolved mass flows, especially for Al, Fe and Mn.  
397 Similarly, the dissolved mass flows of As, Cd, Cr, Cu and Mo are generally of the same



398 magnitude as total mass flows. The total mass flows of most metals (As, Cr, Cu, Fe, Mo, Pb,  
399 V and Zn) were higher in the 2013 campaign than in the 2012 campaign (median: 5 times  
400 higher). ~~Furthermore, This net export of several metals from the Zaamar site was shown in~~  
401 ~~Thorslund et al. (2012); quantified from reported monthly average data. These mass flows of~~  
402 ~~metals at the same locations during summer or autumn months of 2005, 2006 and 2008, in~~  
403 ~~many cases showing were often even higher mass flows~~ than during the present 2013  
404 campaigns.

### 405 **4.3 Modelling results**

#### 406 **4.3.1 Comparing observations and model predictions**

407 Fig. 4 compares the measured and modeled results for the dissolved fraction (percentage) of  
408 considered metals and sampling locations in the (a) 2012 and (b) 2013 campaign. Cr, Cu and  
409 Mo were always predicted to be 100 % dissolved, whereas Mn was predicted to be 100 %  
410 precipitated throughout the study, although measured dissolved fractions changed with  
411 location (see Appendix B for values). Due to the ~~lack of static~~ model ~~sensitivity output~~ for  
412 these metals, they are excluded from Fig. 4 but further discussed below (Sect. 5). Model  
413 predictions for Cd did not always correlate well with measured data (30 %, average difference  
414 between measured and modelled results). However, for all other metals (Al, As, Fe, Pb, V and  
415 Zn; Fig. 4), model predictions in both campaign years agreed well with measurements (within  
416 a 20 % difference between measured and modelled results) for the majority of metals and  
417 locations (67 % of all data points in 2012 and 76 % in 2013), with larger discrepancies  
418 between the measured and modelled results in 2012 than in 2013. The overall best agreement  
419 was for Al and Fe (< 5 % average difference between measured and modelled results).

#### 420 **4.3.2 Speciation of metals**

421 Refined speciation modelling results for the Tuul River ~~around Zaamar Goldfield focus reach~~  
422 from 2012 are shown in Fig. 5 and the results from the more extensive sampling campaign in  
423 2013 are shown in Fig. 6 a to g. Here, the measured 'dissolved' fraction is comparable to the

424 sum of the modelled two fractions: ‘dissolved inorganic’ and ‘bound to DOM’, while the  
425 modelled ‘sorbed’ and ‘precipitated’ fractions together correspond to the measured ‘total’  
426 fraction (unfiltered samples). Due to high measured alkalinity in some locations in 2013, a  
427 test run for these locations where alkalinity was lowered to the 2012 values was performed.  
428 However, changing the alkalinity values in the model input did not significantly change the  
429 speciation of selected metals, indicating a low sensitivity to this parameter.

430  
431 Precipitation of gibbsite and ferrihydrite was predicted as the dominant control of Al and Fe,  
432 with the particulate fraction generally reaching 90-100 %, for both campaign years. The only  
433 exception to these results were predictions for the most upstream Tuul river locations (T2, T3)  
434 sampled in 2013 (Fig. 6), ~~where showing~~ 40-50 % ~~were predicted~~ to occur as soluble organic  
435 complexes (~~b~~Bound to DOC). Compared to the other locations, where only minor fractions of  
436 Fe (up to 5 %) were predicted to exist as complexes with organic matter, pH was the main  
437 difference (being lower at the upstream locations), potentially limiting precipitation.

438 Adsorption to ferrihydrite and gibbsite controlled the speciation of the rest of the metals to  
439 various degrees according to the modeling results, mainly limiting the dissolution of V, Pb  
440 and Zn. The latter was consistently predicted to sorb only to gibbsite, on average showing  
441 adsorbed fractions of 50 % (in 2013) and 80 % (in 2012). The overall highest sorbed fractions  
442 in 2013 was predicted for the Sharyngol River and the ponds, with all Zn being sorbed at  
443 location P4. Pb and V were predicted to sorb to ferrihydrite, on average by 40 % (2012) to 60  
444 % (2013). The sorbed fraction reached over 70 % in several locations, with pond P4 showing  
445 the overall highest results. At location T6 (2012), Pb was predicted to sorb more to gibbsite  
446 than to ferrihydrite. This was also seen for V at location P4, although all other locations  
447 showed sorption to ferrihydrite only. These locations had a very high measured particulate Al  
448 concentration (see Fig. 2 and SI). Contrasting cases of low sorbed and high dissolved fractions  
449 of V, Pb and Zn includes one of the ponds (P1) and the most upstream Tuul River locations  
450 (T2,T3).

451

452 Dissolved inorganic forms (mainly  $\text{HAsO}_4^{2-}$ ) were predicted to dominate almost consistently  
453 for As in both years, on average governing its solubility by 75 %. However, the different  
454 ponds locations showed varying predictions a wide range of predicted conditions, both  
455 including the highest (P1; 90 %) and lowest (P4; 2 %) soluble fractions, in the latter case with  
456 sorption to ferrihydrite limiting the solubility. ~~Contradicting~~ In contrast to the 2013  
457 predictions, V was in 2012 dominated by the dissolved inorganic fraction, hydrogen vanadate  
458 ( $\text{HVO}_4^{2-}$ ).

459 Complexation with organic matter largely governed the solubility of Cd, in both years, where  
460 on average by 63 % (2013) to 75 % (2012) was modelled as “Bound to DOM”. Pb and Zn  
461 were also predicted to bind to DOC, on average by 50 % and 30 %, respectively, in the 2013  
462 campaign and by approximately 15 % less in the 2012 campaign compared to 2013. Overall, a  
463 comparison of the speciation between the two field campaigns suggests that Cd, Pb and Zn  
464 had higher average solubility during 2013 (i.e., a larger quantity modelled as either dissolved  
465 inorganic and/or bound to DOM), with 5 % (Cd), 15 % (Pb) and 25 % (Zn). The impact of  
466 When the DOC concentrations were increased by 50% in the model, in order to investigate the  
467 influence of the uncertainty in DOC concentrations, an increased fraction of all investigated  
468 metals was modelled as dissolved, with the greatest impacts on Fe, Pb and Zn solubility, on  
469 average increasing by 65 %, 40 % and 30 % respectively, but with values reaching over 80 %  
470 increase for all these metals compared to site specific conditions. Scenario simulations  
471 assuming 0% DOC for Tuul River locations (T2, T3, T4, T6b, T7) decreased the agreement  
472 between measured and modeled results for V and Pb. When DOC was accounted for,  
473 differences between measured and modeled dissolved fractions were 9 % (V) and 3 % (Pb).  
474 Without DOC this difference increased to 28 % (V) respectively 53 % (Pb).

475  
476 The model simulations where pH was lowered to 6 and 3.5 generally increased the dissolved  
477 fraction of most metals. At pH 3.5, 100 % dissolved fractions of all previously adsorbed or  
478 precipitated metals was predicted, compared to their speciation at site-specific pH. Lowering

479 the pH to 6 had a large impact on the modelling results for Al, Cd, Fe and Zn, where a larger  
480 fraction was modelled as dissolved compared to at site-specific pH.

481 Zn was the element most influenced by the lower pH, where the fraction modelled as  
482 dissolved was on average twice as large, and in some sites, especially in the ponds, as much as  
483 five times higher compared to at site-specific pH. Ferrihydrite and gibbsite followed the same  
484 pattern, where a model run with pH 6 results in a much higher fraction modelled as dissolved  
485 compared to at ambient pH, up to 25 times higher for the river locations and even higher in  
486 ponds. However, due to the small dissolved fractions in the original model runs for Al and Fe,  
487 this overall impact is minor. For As, V and Pb, the fraction modelled as dissolved instead  
488 decreased slightly by changing the pH to 6, due to increased sorption to ferrihydrite.

489

## 490 **5 Discussion**

491 The main chemical parameter controlling the solubility of metals in aqueous systems is often  
492 considered to be pH (e.g., Bourg and Loch, 1995). The agreement between the present  
493 observations of high concentrations of metals in suspension and the predicted precipitation  
494 and/or sorption controls shows that dissolution is generally limited for several metals under  
495 the alkaline conditions that prevail in the studied region. The pH 3.5 modelling scenario  
496 simulates pH conditions common at many well-studied acid mine drainage sites (e.g., Elliot et  
497 al., 1998 and Saria et al., 2006). Under such conditions, practically all metals are dissolved.  
498 The model predictions of the pH 6 scenario compared to site conditions also changed the  
499 speciation of the metals. The substantial difference on the fraction of Zn modelled as  
500 dissolved between the site conditions and pH 6 suggest that this metal is very sensitive to  
501 fluctuations in pH. This finding agrees with results from Chen et al., (1997), for instance, who  
502 also showed Zn to be pH sensitive, with a significantly decreasing solubility above pH 6.5, at  
503 which all dissolved Zn was removed from solution due to adsorption.

504 Adsorption is a main process controlling metal solubility in natural systems (e.g., Zhao et al.,  
505 2011). The high affinity of 'divalent base metals', including Cd, Cu, Pb and Zn, to adsorb to

506 solid phases such as Al and Fe hydroxides is common (e.g., Early 1999). Our modelling  
507 results indicated that adsorption to Al (gibbsite) was an important controlling factor only for  
508 Cd and Zn solubilities, with the greatest impact on Zn and a minor influence on Cd.  
509 Furthermore, because Pb and V were predicted to adsorb to gibbsite instead of ferrihydrite,  
510 when Al concentrations reached similar or higher concentrations as Fe, gibbsite could also  
511 control Pb and V solubility. Studies of the adsorption to gibbsite under high-pH conditions are  
512 not abundant. However, Weerasooriya et al. (2001) showed sorption of Pb to gibbsite in the  
513 same range as predicted here, with up to 50 % sorption to gibbsite at pH 9, which supports our  
514 results. Otherwise, the sorption of metals to ferrihydrite is commonly reported (e.g., Shultz et  
515 al., 1987, Jung et al., 2005 and Sanchez-España et al., 2006) and was here predicted to be the  
516 main solid for adsorption Pb and V, and in some locations also for As. The degrees of sorption  
517 of these metals were all predicted to increase when the input pH was changed to 6, suggesting,  
518 in agreement with literature, that these metals are less soluble at pH 6 than at site conditions  
519 (e.g. Dzombak and Morel 1990). However, the results from the predictions at pH 3.5, which  
520 show a complete dissolution of previously sorbed metals, indicate that sorption is not an active  
521 control under acidic mine drainage conditions. Several other studies have shown the highest  
522 adsorption of these metals to ferrihydrite at circum-neutral pH. For example, Sanchez-España  
523 et al. (2006) showed 90-99 % adsorption of As and Pb to ferrihydrite within the pH range 7-8.  
524 Moreover, Jung et al. (2005) indicated 95 % adsorption of Cd, Pb and Zn onto ferrihydrite at  
525 pH 7. These findings suggest that adsorption onto ferrihydrite mainly limits dissolved forms of  
526 these metals at circum-neutral pH, but adsorption still occurs at the very high pH conditions  
527 predicted in our study, with up to over 70 % sorption of Pb and V to ferrihydrite.

528  
529 For As, the analytical results show that the dissolved fraction is generally dominating (Fig 2).  
530 This is in agreement with the modelling results, which indicate that it is the dissolved  
531 inorganic fraction ( $\text{HAsO}_4^{2-}$ ) that is the dominating form (Fig 5 and 6). This indicates a higher  
532 bioavailability of this metal compared to the others. As is well known to be highly soluble in  
533 alkaline conditions (e.g., Early 1999), especially in combination with non-humid climates

534 (Smedley and Kinniburgh 2002), which agrees with our results. Based on a similar modelling  
535 approach as in the present study, Wällstedt et al. (2010) suggested that the dissolved inorganic  
536 fraction was the dominating form of As in streams with pH above 6.9. Furthermore, because  
537 dissolved As concentrations reached concentrations above those commonly found in  
538 freshwaters (Smedley and Kinniburgh 2002) and health risk-based guideline values (WHO) in  
539 several locations in the present study, this metal is of toxic concern in the study area. Recent  
540 papers on metal contamination in Mongolia (Hofmann et al., 2014 and Pfeiffer et al., 2014)  
541 also shows high dissolved As concentrations in several high pH regions, with elevated values  
542 in areas of gold mines (including the Zaamar Goldfield), highlighting this problem.

543 The model results also suggested that DOC influenced the speciation of several metals. Our  
544 scenario results showing that the model performance was considerably lower assuming zero  
545 DOC concentrations instead of site-specific values are consistent with those of Ahmed et al.  
546 (2014). The study highlights that organic matter concentrations can have large impact on  
547 metal speciation in non-acidic systems, due to increased negative charge on the humic  
548 molecules, which enhances the complexation capacity with the positively charged metal ions.  
549 With site-specific DOC concentrations, metal-organic complexation was modelled as the  
550 main controlling factor for Cd solubility and DOC also influenced the solubility of Pb and Zn.  
551 Many studies (e.g., Christensen et al., 1996, Hagedorn et al., 2000 and Sauvé et al., 2000) have  
552 suggested that DOC is an important controlling factor for metal transport and fate in natural  
553 systems. A modelling approach by Weng et al. (2002) showed that complexation with organic  
554 matter could lead to dissolved concentrations of Pb of up to two orders of magnitude greater  
555 than those without DOC, especially in alkaline conditions, and with significant effects also on  
556 the solubility of Cd and Zn. Antoniadis and Alloway (2002), however, found that  
557 complexation with DOC significantly increased the dissolved concentrations of Cd and Zn, a  
558 result that agrees with the model results from this study. Additionally, the binding of Fe and  
559 Al to organic matter has been shown to affect the binding of other metals as well. High  
560 concentrations of Fe and Al were shown by Tipping et al. (2002) to dominate the space of the  
561 organic matter, thereby increasing the dissolved concentrations of other metals, which could

562 no longer remain in a complex with the organic material. This condition was observed  
563 throughout for Fe in our modelled system; when DOC concentrations were increased by 50 %,  
564 Fe-organic complexation also increased, by between 50 % and 80 %, while a larger fraction of  
565 metals previously modelled as adsorbed to ferrihydrite was modelled as dissolved. If site-  
566 specific DOC concentrations were higher than our assumed values for the 2012 campaign,  
567 more metal-organic complexes could exist in our system than what was predicted, suggesting  
568 that the systematic under-prediction of the dissolved fraction for many metals in 2012 (Fig.  
569 4a) could be related to DOC. Several studies (e.g., Schelker et al., 2012, and Raymond and  
570 Saiers 2010) have shown that DOC concentrations fluctuate up to several 100 % due to land  
571 use changes (deforestation) and storm events, for instance. Because data on DOC variability in  
572 the studied region is scarce (Yoshioka et al., 2002), it is possible that real DOC concentrations  
573 in 2012 were higher than in 2013.

574 As noted in the results (sect. 4.3), the modelled speciation of Cr, Cu, Mn and Mo did not agree  
575 well with the measured fractionation. A possible reason for this disparity could be the impact  
576 of adsorption onto precipitates not included in the model. Apatites, a group of phosphate  
577 minerals, have commonly been suggested to be the main solids limiting the dissolved form of  
578 several metals in natural systems (e.g., Chen et al., 1997). Notably, hydroxyapatite, which is a  
579 natural calcium phosphate mineral within the apatite group, may be an important solid  
580 providing adsorption sites in our study region, because it was oversaturated (i.e., would  
581 precipitate if added as a possible solid phase) according to the model throughout the modelled  
582 locations. The measured concentrations of particulate calcium and phosphorous, which are  
583 chemical constituents of the mineral, were also considerable in the Tuul River, suggesting that  
584 the mineral may be present in the system. However, it would be premature to add this mineral  
585 to the model as a possible solid for adsorption due to the current lack of an adsorption  
586 database for this phase. Nevertheless, several previous studies (e.g., Corami et al., 2008, Chen  
587 et al., 2010, Feng et al., 2010 and Corami et al., 2012) have pointed to the importance of this  
588 solid for the adsorption of metals, including Cr, Cu and Mo. For example, the adsorption of Cr  
589 to hydroxyapatite was shown experimentally by Asgari et al. (2012) to remove high fractions

590 of dissolved Cr up to a pH of 11. Hence, hydroxyapatite may serve as an active control on  
591 several metals, including Cr, Cu and Mo, in non-acidic systems.

592 Linking the results from the analytical fractionation and the speciation modelling with the  
593 measured concentrations and mass flow quantifications highlights the strong correlation  
594 between the modelled forms of precipitated Fe and Al and their high impact on suspended to  
595 total transport. The potential capacity of sediments to hold much more metals than a  
596 corresponding volume of water is well known (e.g. Horowitz, 1991). The combined effects of  
597 mining activities that stir up metal-rich bottom sediments, and the non-acidic environment that  
598 cause precipitation of Al and Fe and enhance adsorption of several other metals, lead to an  
599 overall large export of several metals in suspension from the site. This situation is in line with  
600 previous site assessments (Thorslund et al., 2012), suggesting a net contribution of metal loads  
601 transported from the Zaamar Goldfield compared to the natural mass flows. Because the  
602 concentrations of the metals did not vary as much as the discharges, the discharge would be  
603 the main factor controlling the magnitude of the mass flows. The impact of discharge on  
604 pollutant loads was also noted by Basu et al. (2010).

605  
606 Considering the combined influences of land use alterations (expansion of mining areas) and  
607 projected climate changes (increased frequency of peak flow events; Altansukh and Davaa  
608 2011), which will likely result in increased discharge and erosion in the Lake Baikal Drainage  
609 Basin, one can expect that the transport of metals from the Zaamar site to the connected river  
610 system will also increase. Increasing organic matter concentrations have also been found to  
611 correlate with increasing discharge (e.g. Lewis and Grant 1979), which could enhance  
612 solubility for several metals in suspension. The transport of metals to downstream regions,  
613 where geochemical conditions might be different (e.g., Yoshioka et al., 2002) could  
614 potentially also increase the solubility and bioavailability of metals in suspension. This does  
615 not only apply for this system, but can be of general relevance for spreading and fate of metals  
616 in non-acidic systems. This potential highlights the need for further studies focusing on the  
617 large-scale implications of coupled hydrodynamic (governing the magnitude of suspended



618 sediment transport) and geochemical (governing the mobility of metals between the sediment  
619 and water phases) processes.

620

## 621 **6 Conclusions**

622 Under non-acidic conditions, riverine suspended mass flows typically constitute the dominant  
623 component of total mass flows, as observed during our snapshot measurements in the Tuul  
624 River. Total mass flows showed net increases across the Zaamar Goldfield, reflecting the  
625 export of several metals (Al, Cd, Fe, Mn, Pb and V) from this mining site to the downstream  
626 river system. The main geochemical control limiting the solubility of metals in this non-acidic  
627 system, identified through speciation modeling, was the precipitation of ferrihydrite and  
628 gibbsite, which removed between 90 and 100 % of the Fe and Al from solution. This effect  
629 additionally influenced the speciation of V, Pb and Zn because their solubilities are to large  
630 extent controlled by sorption onto these solids; with sorption to ferrihydrite removing between  
631 40 to 60% of V and Pb from solution and sorption to gibbsite removing up to 80% of Zn from  
632 solution. Observations and model estimations suggest considerable impacts of sorption for  
633 prevailing conditions in rivers and in surface water ponds.

634

635 Simulations also suggest that organic matter constitutes a dominant control keeping several  
636 metals (Cd, Pb and Zn) in solution. In non-acidic environments, most metals have relatively  
637 low solubilities in the absence of DOC and the predictions where DOC concentrations were  
638 increased highlight the possibility of considerably increased metal-organic complexation for  
639 several metals, in particular Fe, Pb and Zn. In non-acidic systems, the seasonality of DOC  
640 concentrations (which can vary by several 100 %) can therefore have a major influence on the  
641 spreading and toxicity of these metals and need to be accounted for in both field  
642 measurements and speciation modeling. The solubility of these metals could change  
643 considerably in response to climate and land use changes that impact DOC concentrations,  
644 such as the increasing frequency of storm events, agricultural expansion and deforestation.

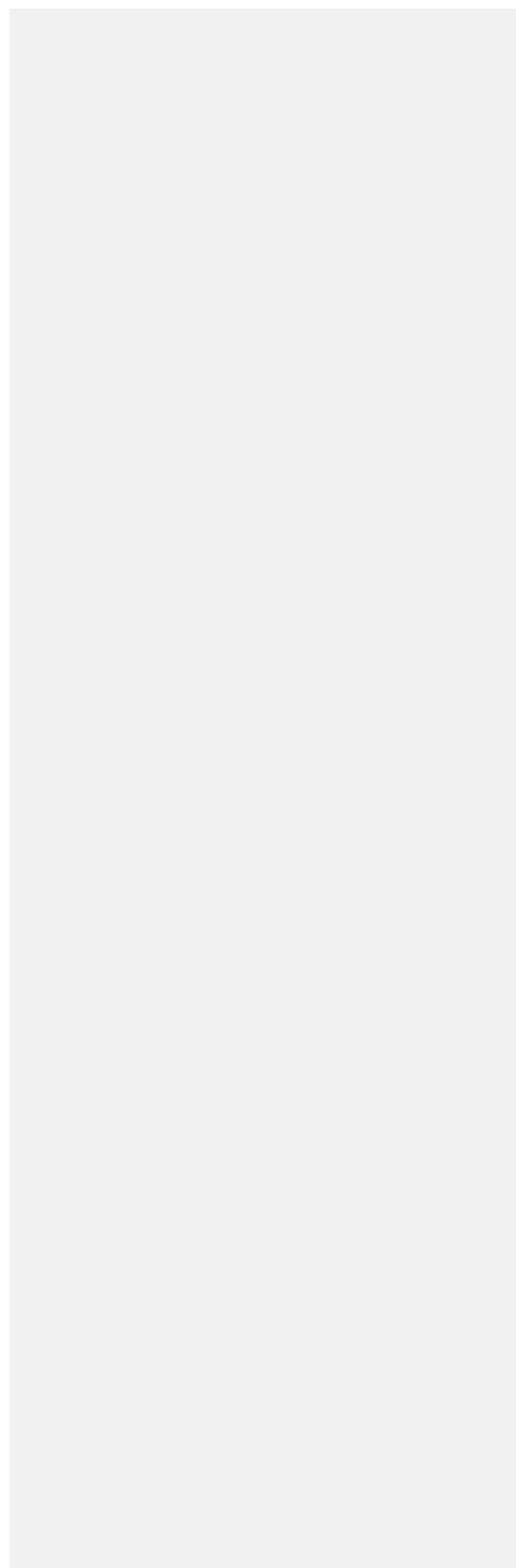
Formatted: Indent: Left: 0", First line: 0"

645 Under present site conditions, As was the only metal where the dissolved form was  
646 dominating throughout most locations. It was predominantly modelled to occur in its  
647 dissolved inorganic form ( $\text{HAsO}_4^{2-}$ ) and showed measured dissolved concentrations above  
648 health risk-based guideline values in several locations. This metal is thus of primary toxic  
649 concern in the Upper Lake Baikal Drainage Basin.

650 For most metals, the simulated results of dissolution fractions generally agreed well  
651 (differences within 20 % for the dissolved fractions) with observations in the considered  
652 systems. However, with this current model approach, predictions of Cr, Cu, Mn, Mo and Cd  
653 (in some locations), were not satisfactory. An identified possible reason for this discrepancy is  
654 that the model do not account for the influence of sorption to hydroxyapatite, an apatite  
655 mineral known to have high sorption capacity. Nevertheless, no adsorption database is  
656 currently available for hydroxyapatite, which hinders appropriate sorption quantification. The  
657 potential importance of this mineral for metal partitioning under non-acidic conditions in  
658 general and for the investigated Tuul River in particular is emphasised by the fact that this  
659 mineral's constituents were observed on site, with conditions being favourable for its  
660 precipitation.

661 Overall, the model approach used in this application that accounted for surface complexation,  
662 including binding to common solids and dissolved organic matter, worked well for 76 % of  
663 the large number of simulated metals. Further, the modelled speciation for the Tuul River  
664 focus reach supports the conducted load estimations and the export of metal enriched  
665 suspended sediments from the Zaamar site to downstream regions. Although further model  
666 development is needed, for instance developing sorption databases, the present results show  
667 that the applicability of this approach can work well to both surface and river systems in non-  
668 acidic systems, is identified to work well. However, ~~w~~We suggest that the combination of  
669 transport quantifications and ~~a~~this geochemical modelling need to be applied in other non-  
670 acidic systems with different geochemical conditions, to approach can further increase the  
671 understanding of controls governing metal spreading and fate.

672



674

## **Appendix A**

675

**Table A1. Maximum permissible concentration levels (µg/l) in drinking water according to the World Health Organization (WHO 2006) and the Mongolian State Standard (AATA 2008).**

676

677

	<b>Al</b>	<b>As</b>	<b>Cd</b>	<b>Cr</b>	<b>Cu</b>	<b>Fe</b>	<b>Mn</b>	<b>Mo</b>	<b>Pb</b>	<b>V</b>	<b>Zn</b>
<b>WHO</b>	200	10	3.00	50	2000	300	400	70	10	200	3000
<b>Mongolian</b>	500	10	-	-	-	300	100	-	10	-	5000

678

679

Formatted: Heading 1, Indent: Left: 0.01", Space After: 0 pt, Line spacing: single

680  
681  
682  
683

**Appendix B**

Formatted: Heading 1, Indent: Left: 0.01", Space After: 0 pt, Line spacing: single

**Table B1. Comparison of measured and modelled dissolved fractions of the selected metals in 2012.**

<b>% Dissolved Measured</b>	<b>Al</b>	<b>As</b>	<b>Cd</b>	<b>Cr</b>	<b>Cu</b>	<b>Fe</b>	<b>Mn</b>	<b>Mo</b>	<b>Pb</b>	<b>V</b>	<b>Zn</b>
T5	0.3	96.5	NA	NA	67.5	3.5	6.0	84.5	72.3	88.7	57.4
T5a	0.3	93.4	NA	10.0	26.1	2.4	2.0	33.5	NA	73.1	24.7
T5b	3.6	85.7	87.1	39.4	NA	3.7	89.1	88.9	NA	78.0	28.1
T6	1.1	NA	67.5	21.2	NA	2.3	2.6	41.2	12.1	62.8	44.5
T6a	4.0	92.2	86.9	35.1	NA	2.7	4.5	80.5	NA	82.2	64.4
<b>% Dissolved Modelled</b>	<b>Al</b>	<b>As</b>	<b>Cd</b>	<b>Cr</b>	<b>Cu</b>	<b>Fe</b>	<b>Mn</b>	<b>Mo</b>	<b>Pb</b>	<b>V</b>	<b>Zn</b>
T5	2.63	72.3	NA	NA	100	2.54	0.00	100	48.4	55.0	45.3
T5a	1.77	39.8	NA	100	99.8	0.21	0.00	100	NA	37.1	5.76
T5b	1.29	94.5	90.2	100	NA	0.82	0.00	100	NA	75.6	23.5
T6	0.05	NA	53.0	100	NA	0.46	0.00	100	19.4	52.8	3.08
T6a	0.78	98.6	91.4	100	NA	2.03	0.00	100	NA	89.2	24.2

684  
685  
686

**Table B2. Comparison of measured and modelled dissolved fractions of the selected metals in 2013.**

<b>% Dissolved Measured</b>	<b>Al</b>	<b>As</b>	<b>Cd</b>	<b>Cr</b>	<b>Cu</b>	<b>Fe</b>	<b>Mn</b>	<b>Mo</b>	<b>Pb</b>	<b>V</b>	<b>Zn</b>
T2	27.6	NA	10.0	NA	NA	30.8	53.2	NA	86.0	63.9	66.4
T3	18.5	41.6	10.0	NA	NA	23.8	59.6	NA	55.5	62.1	100.0
T4	1.7	NA	100.0	NA	NA	5.8	12.0	NA	33.9	46.0	46.6
T5	2.49	NA	NA	66.8	55.2	8.8	10.6	NA	53.4	40.7	70.2
T5a	2.55	NA	45.1	92.8	83.7	6.7	42.3	NA	57.2	64.9	48.3
T5b	6.07	NA	NA	74.8	69.9	7.5	25.1	82.0	50.9	57.5	105
T6	0.92	76.4	76	102	62.3	2.2	15.6	77.4	40.7	45.0	31.0
T6a	11.9	NA	NA	75.4	83.6	3.7	11.7	NA	37.8	45.8	48.7

T6b	<u>6.9</u>	<u>NA</u>	<u>10.0</u>	<u>NA</u>	<u>NA</u>	<u>10.6</u>	<u>21.0</u>	<u>NA</u>	<u>51.8</u>	<u>50.0</u>	<u>68.4</u>
T7	<u>1.9</u>	<u>NA</u>	<u>67.9</u>	<u>NA</u>	<u>NA</u>	<u>2.8</u>	<u>3.8</u>	<u>NA</u>	<u>49.6</u>	<u>48.1</u>	<u>79.4</u>
S1	<u>4.77</u>	<u>NA</u>	<u>NA</u>	<u>NA</u>	<u>NA</u>	<u>12.7</u>	<u>23.2</u>	<u>94.0</u>	<u>91.6</u>	<u>50.1</u>	<u>59.6</u>
S2	<u>1.02</u>	<u>91.9</u>	<u>NA</u>	<u>NA</u>	<u>NA</u>	<u>1.70</u>	<u>1.78</u>	<u>80.7</u>	<u>45.8</u>	<u>37.4</u>	<u>19.0</u>
S3	<u>0.80</u>	<u>NA</u>	<u>NA</u>	<u>NA</u>	<u>NA</u>	<u>0.97</u>	<u>1.00</u>	<u>87.5</u>	<u>28.6</u>	<u>31.9</u>	<u>16.0</u>
S5	<u>0.38</u>	<u>NA</u>	<u>NA</u>	<u>NA</u>	<u>NA</u>	<u>0.44</u>	<u>1.82</u>	<u>NA</u>	<u>29.8</u>	<u>35.2</u>	<u>18.9</u>
P1	<u>17.9</u>	<u>69.5</u>	<u>NA</u>	<u>NA</u>	<u>NA</u>	<u>6.04</u>	<u>NA</u>	<u>97.0</u>	<u>73.1</u>	<u>61.0</u>	<u>60.8</u>
P3	<u>0.42</u>	<u>85.5</u>	<u>59.2</u>	<u>NA</u>	<u>NA</u>	<u>3.10</u>	<u>12.7</u>	<u>NA</u>	<u>40.1</u>	<u>39.7</u>	<u>49.0</u>
P5	<u>0.05</u>	<u>31.9</u>	<u>0.64</u>	<u>NA</u>	<u>NA</u>	<u>0.03</u>	<u>0.07</u>	<u>NA</u>	<u>1.54</u>	<u>2.74</u>	<u>9.08</u>
<b>% Dissolved Modelled</b>	<b>Al</b>	<b>As</b>	<b>Cd</b>	<b>Cr</b>	<b>Cu</b>	<b>Fe</b>	<b>Mn</b>	<b>Mo</b>	<b>Pb</b>	<b>V</b>	<b>Zn</b>
T2	<u>7.84</u>	<u>NA</u>	<u>99.8</u>	<u>NA</u>	<u>NA</u>	<u>50.6</u>	<u>0.50</u>	<u>NA</u>	<u>62.2</u>	<u>53.7</u>	<u>98.8</u>
T3	<u>4.82</u>	<u>76.7</u>	<u>99.7</u>	<u>NA</u>	<u>NA</u>	<u>38.6</u>	<u>0.25</u>	<u>NA</u>	<u>57.8</u>	<u>53.4</u>	<u>97.9</u>
T4	<u>0</u>	<u>NA</u>	<u>89.0</u>	<u>NA</u>	<u>NA</u>	<u>2.85</u>	<u>0.00</u>	<u>NA</u>	<u>40.3</u>	<u>22.4</u>	<u>38.3</u>
T5	<u>1.54</u>	<u>NA</u>	<u>NA</u>	<u>100</u>	<u>100</u>	<u>4.27</u>	<u>0.00</u>	<u>NA</u>	<u>71.0</u>	<u>63.9</u>	<u>71.9</u>
T5a	<u>0.60</u>	<u>NA</u>	<u>97.0</u>	<u>100</u>	<u>100</u>	<u>7.23</u>	<u>0.00</u>	<u>NA</u>	<u>67.0</u>	<u>56.6</u>	<u>75.0</u>
T5b	<u>0.29</u>	<u>NA</u>	<u>NA</u>	<u>100</u>	<u>100</u>	<u>2.66</u>	<u>0.00</u>	<u>100</u>	<u>58.0</u>	<u>49.1</u>	<u>51.0</u>
T6	<u>0.63</u>	<u>85.0</u>	<u>91.0</u>	<u>100</u>	<u>100</u>	<u>1.21</u>	<u>0.00</u>	<u>100</u>	<u>41.1</u>	<u>53.7</u>	<u>32.0</u>
T6a	<u>0.29</u>	<u>NA</u>	<u>NA</u>	<u>100</u>	<u>100</u>	<u>1.58</u>	<u>0.00</u>	<u>NA</u>	<u>45.2</u>	<u>49.7</u>	<u>21.0</u>
T6b	<u>0.63</u>	<u>NA</u>	<u>95.8</u>	<u>NA</u>	<u>NA</u>	<u>7.34</u>	<u>0.00</u>	<u>NA</u>	<u>64.4</u>	<u>31.0</u>	<u>66.3</u>
T7	<u>0.20</u>	<u>NA</u>	<u>89.3</u>	<u>NA</u>	<u>NA</u>	<u>1.33</u>	<u>0.00</u>	<u>NA</u>	<u>38.5</u>	<u>17.5</u>	<u>36.4</u>
S1	<u>0.73</u>	<u>NA</u>	<u>NA</u>	<u>NA</u>	<u>NA</u>	<u>9.16</u>	<u>0.00</u>	<u>100</u>	<u>68.9</u>	<u>42.9</u>	<u>53.0</u>
S2	<u>0.13</u>	<u>88.9</u>	<u>NA</u>	<u>NA</u>	<u>NA</u>	<u>1.69</u>	<u>0.00</u>	<u>100</u>	<u>33.1</u>	<u>47.6</u>	<u>11.5</u>
S3	<u>0.08</u>	<u>NA</u>	<u>NA</u>	<u>NA</u>	<u>NA</u>	<u>0.95</u>	<u>0.00</u>	<u>100</u>	<u>20.6</u>	<u>9.08</u>	<u>14.9</u>
S5	<u>0.05</u>	<u>NA</u>	<u>NA</u>	<u>NA</u>	<u>NA</u>	<u>0.55</u>	<u>0.00</u>	<u>NA</u>	<u>11.7</u>	<u>8.12</u>	<u>7.25</u>
P1	<u>0.97</u>	<u>98.3</u>	<u>NA</u>	<u>NA</u>	<u>NA</u>	<u>4.28</u>	<u>NA</u>	<u>100</u>	<u>100</u>	<u>95.1</u>	<u>99.9</u>
P3	<u>0.22</u>	<u>42.0</u>	<u>85.4</u>	<u>NA</u>	<u>NA</u>	<u>2.61</u>	<u>0.00</u>	<u>NA</u>	<u>36.0</u>	<u>16.0</u>	<u>19.2</u>
P4	<u>0.01</u>	<u>11.5</u>	<u>4.08</u>	<u>NA</u>	<u>NA</u>	<u>0.02</u>	<u>0.00</u>	<u>NA</u>	<u>0.62</u>	<u>3.13</u>	<u>0.17</u>

687

## Author contribution

J. Thorslund did model simulations and manuscript preparation, with contributions from all coauthors. J. Thorslund, J. Jarsjö and S. Chalov developed research ideas, including field preparations, measurements and modelling approach. T Wällstedt was responsible for modelling aspects, including parameter settings. M. Mörtz was responsible for analytical methods, sampling handling and analysis. M. Lychagin contributed to geochemical interpretation.

## Acknowledgements

This research was conducted within the project *Basin-scale hydrological spreading of pollutants and wetland opportunities for reducing them under different hydroclimatic and other regional conditions*, funded by the Swedish Research Council Formas (project 2012-790). This study is also part of the project *Hydroclimatic and ecohydrological changes of the Lake Baikal drainage basin*, financially supported by a travel grant from the Faculty of Science, Stockholm University. This work was additionally implemented under the support of the Russian–Mongolian biological expedition RAS-MAS with a Russian geographical society grant ‘Expedition Selenga–Baikal’ from the Russian Foundation for Basic Research (project nr 12-05-00069-a, 12-05-33090).

## References

- AATA International Inc. Social and Environmental Impact Assessment. Big Bend Placer Gold Mining Project, Mongolia. Denver, Colorado, USA. 2008.
- [Ahmed, I.A.M., Hamilton-Taylor, J., Bierzoza, M., Zhang, H. and Davidson, W.: Improving and testing geochemical speciation predictions of metal ions in natural waters. \*Water Research\*, 67, 276-291, 2014.](#)
- Alexeevsky NI., Chalov, R.S., Berkovich, K.M. and Chalov, S.R.: Channel changes in largest Russian rivers: natural and anthropogenic effects, *International Journal of River Basin Management*, 11:2, 175-191, DOI: 10.1080/15715124.2013.814660, 2013.
- Altansukh, O. and Davaa, G.: Application of Index Analysis to Evaluate the Water Quality of the Tuul River in Mongolia, *Journal of Water Resource and Protection*, 03, 398–414, 2011.
- Antoniadis, V. and Alloway, B.J.: The role of dissolved organic carbon in the mobility of Cd, Ni and Zn in sewage sludgeamended soils, *Environ. Pollut.*, 117, 515–521, 2002.

- Asgari G., Rahmani A.R., Faradmal J., and Seid Mohammadi AM.: Kinetic and isotherm of hexavalent chromium adsorption onto nano hydroxyapatite, *Journal of research in health sciences*, 12(1), 2012.
- Balistreri, L.S., Seal, R.R., Piatak, N.M., and Paul, B.: Assessing the concentration, speciation, and toxicity of dissolved metals during mixing of acid-mine drainage and ambient river water downstream of the Elizabeth Copper Mine, Vermont, USA, *Appl Geochem.*, 22(5), 930–952, 2007.
- Basu, N.B., Destouni, G., Jawitz, J.W., Thompson, S.E., Loukinova, N.V., Darracq, A., Zanardo, S., Yaeger, M., Sivapalan, M., Rinaldo, A., and Rao, P.S.C.: Nutrient loads exported from managed catchments reveal emergent biogeochemical stationarity, *Geophysical Research Letters*, 37, 2010.
- Bourg, A.C.M., and Loch, J.P.G.: Mobilization of Metals as Affected by pH and Redox Conditions, in: Salomons, P.D.W., Stigliani, P.D.W.M. (Eds.), *Biogeochemistry of Pollutants in Soils and Sediments*, Environmental Science. Springer Berlin Heidelberg, 87–102, 1995.
- Butler, B.A., Ranville, J.F., and Ross, P.E.: Observed and modeled seasonal trends in dissolved and particulate Cu, Fe, Mn, and Zn in a mining-impacted stream, *Water Res.*, 42(12), 3135–3145, 2008.
- Butler, B.A., Ranville, J.F., and Ross, P.E.: Spatial variations in the fate and transport of metals in a mining-influenced stream, North Fork Clear Creek, Colorado. *Science of the Total Environment*, 407, 6223–6234, 2009.
- Bykov, V.D., and Vasil'ev, A. V.: Hydrometry (in Russian), *Gidrometeoizdat*, Leningrad. 1972.
- Caruso, B.S., Cox, T.J., Runkel, R.L., Velleux, M.L. Bencala, K.E., Nordstrom, D.K., Julien, P.Y., Butler, B.A., Alpers, C.N., Marion, A. and Smith, K.S.: Metals fate and transport modelling in streams and watersheds: state of the science and USEPA workshop review, *Hydrol Process*, 22, 4011–4021, 2008.
- Chalov S.R., Zavadsky A.S., Belozeroва E.V., Bulacheva M.P., Jarsjö J., Thorslund J., and Yamkhin J.: Suspended and dissolved matter fluxes in the upper Selenga river basin, *Geography Environment Sustainability*, 5(2), 78–94, 2012.
- Chalov, S.R., Jarsjö, J., Kasimov, N.S., Romanchenko, A.O., Pietróń, J., Thorslund, J. and Promakhova, E.V.: Spatio-temporal variation of sediment transport in the Selenga River Basin, Mongolia and Russia, *Environ. Earth Sci*, doi: 10.1007/s12665-014-3106-z, 2014.
- [Chapman, D. 1992. Water quality assessments. Chapman and Hall, New York, NY.](#)
- Chen S.B., Ma Y.B., Chen L., and Xian K.: Adsorption of aqueous Cd<sup>2+</sup>, Pb<sup>2+</sup>, Cu<sup>2+</sup> ions by nano-hydroxyapatite: Single- and multi-metal competitive adsorption study, *Geochem J.*, 44(3), 233–239, 2010.
- Christensen, J.B., Jensen, D.L., and Christensen, T.H.: Effect of dissolved organic carbon on the mobility of cadmium, nickel and zinc in leachate polluted groundwater, *Water Res.*, 30, 3037–3049, 1996.
- Cidu, R., Biddau, R., and Fanfani, L.: Impact of past mining activity on the quality of groundwater in SW Sardinia (Italy), *Journal of Geochemical Exploration*, 100, 125–132, 2009.
- Corami, A., Mignardi, S., and Ferrini, V.: Cadmium removal from single- and multi-metal (Cd plus Pb plus Zn plus Cu) solutions by sorption on hydroxyapatite, *J Colloid Interf Sci.*, 317(2), 402–408, 2008.



- Destouni, G., Persson, K., Prieto, C., and Jarsjö, J.: General quantification of catchment-scale nutrient and pollutant transport through the subsurface to surface and coastal waters. *Environ Sci Technol*, 44, 2048–2055, 2010.
- Dzombak, D.A., and Morel, F.M.M.: Surface Complexation Modeling: Hydrous Ferric Oxide. Wiley-Interscience; 1 edition. ISBN-10: 0471637319, 1990.
- Eary, L.E.: Geochemical and equilibrium trends in mine pit lakes, *Appl Geochem.*, 14(8), 963-987, 1999.
- Elliot, P., Ragusa, S. and Catcheside, D.: Growth of sulfate-reducing bacteria under acidic conditions in an upflow anaerobic bioreactor as a treatment system for acid mine drainage, *Water Res*, 32, 3724–3730, 1998.
- Feng, Y., Gong, J.L., Zeng, G.M., Niu, Y.Q., Zhang, H.Y., Niu, Q.Y., Deng, J.H., and Yan, M.: Adsorption of Cd (II) and Zn (II) from aqueous solutions using magnetic hydroxyapatite nanoparticles as adsorbents, *Chem Eng J.*, 162(2), 487–494, 2010.
- Foster, I.D.L. and Charlesworth, S.M.: Heavy metals in the hydrological cycle: Trends and explanation, *Hydrol Process.*, 10(2), 227–261, 1996.
- Fytianos, K.: Speciation analysis of metals in natural waters: a review, *J AOAC Int.*, 84, 1763–1769, 2001.
- GEMStat.: Global Water Quality Database. <http://www.gemstat.org>. Accessed latest 22 October 2013, 2011.
- Grosbois, C., Schaefer, J., Bril, H., Blanc, G., and Bossy, A.: Deconvolution of trace element (As, Cr, Mo, Th, U) sources and pathways to surface waters of a gold mining-influenced watershed. *Sci Tot Environ.*, 407(6), 2063–2076, 2009.
- Gundersen, P., and Steinnes, E.: Influence of Temporal Variations in River Discharge, pH, Alkalinity and Ca on the Speciation and Concentration of Metals in Some Mining Polluted Rivers, *Aquat Geochem.*, 7, 173–193, 2001.
- Gustafsson, J.P., 2001. Modeling the acid-base properties and metal complexation of humic substances with the Stockholm Humic Model. *Journal of Colloid and Interface Science* 244, 102-112.
- Gustafsson, J.P., Dässon, E., and Bäckström, M.: Towards a consistent geochemical model for prediction of uranium(VI) removal from groundwater by Ferrihydrite, *Appl Geochem.*, 24, 454–462, 2009.
- Gustafsson, J.P.: Visual MINTEQ, version 3.0: a window version of MINTEQA2, version 4.0. <http://www.lwr.kth.se/english/OurSoftware/Vminteq>, 2010.
- Gustafsson et al. Gustafsson, J.P., Persson, I., Oromieh, A.G., van Schaik, J.W.J., Sjöstedt, C., Kleja, D.B., 2014. Chromium(III) Complexation to Natural Organic Matter: Mechanisms and Modeling, *Environ Sci Technol.*, 48, 17531761, 2014.
- Hagedorn, F., Kaiser, K., Feyen, H., and Schleppl, P.: Effects of Redox Conditions and Flow Processes on the Mobility of Dissolved Organic Carbon and Nitrogen in a Forest Soil, *Journal of Environment Quality*, 29, 288, 2000.
- Horowitz, A.J.: A Primer on Sediment-Trace Metal Chemistry (2nd edn) Lewis Publishers, MI. USGS Water Supply Paper: 2277. 1991.

- Hudson-Edwards, K.A.: Sources, mineralogy, chemistry and fate of heavy metal-bearing particles in mining-affected river systems, *Mineral Mag.*, 67, 205–217, 2003.
- Inam, E., Khantotong, S., Kim, K.-W., Tumendemberel, B., Erdenetsetseg, S., and Puntsag, T.: Geochemical distribution of trace element concentrations in the vicinity of Boroo gold mine, Selenge Province, Mongolia, *Environ Geochem Health.*, 33, 57–69, 2011.
- Jung, H.B., Yun, S.T., Mayer, B., Kim, S.O., Park, S.S., and Lee, P.K.: Transport and sediment–water partitioning of trace metals in acid mine drainage: an example from the abandoned Kwangyang Au–Ag mine area, South Korea, *Environ Geol*, 48, 437–449, 2005.
- Karamalidis, A.K., and Dzombak, D.A.: *Surface Complexation Modeling: Gibbsite*. John Wiley Sons ISBN: 978-0-47058768-3, 294 pp. 2010.
- Khai, N.M., Öborn, I., Hillier, S., and Gustafsson, J.P.: Modeling of metal binding in tropical Fluvisols and Acrisols treated with biosolids and wastewater, *Chemosphere*, 70, 1338-1346, 2008.
- Khazheeva, Z. I., Tulokhonov A. K., and Urbazaeva, S. D.: Distribution of metals in water, bottom silt, and on suspensions in the arms of the Selenga delta, *Chem. Sustainable Dev.*, 14, 279–285, 2006.
- Korfali, S.I., and Davies, B.E.: Speciation of metals in sediment and water in a river underlain by limestone: role of carbonate species for purification capacity of rivers, *Adv Environ Res.*, 8, 599–612, 2004.
- Landner, L.: Speciation, Mobility and Bioavailability of Metals in the Environment, in: *Metals in Society and in the Environment*, *Environ Pollut.*, Springer Netherlands, 139–274, 2005.
- Langmuir, D., 1997. *Aqueous Environmental Geochemistry*. Prentice Hall Inc. Simon & Schuster/ A Viacom Company, Upper Saddle River, New Jersey, USA.
- Lee, Y.J., Yun, S.T., Badarch, M., Lee, J., Ayur, O., Kwon, J.S., and Kim, D.M.: Joint Research between Korea and Mongolia on Water Quality and Contamination of Transboundary Watershed in Northern Mongolia. Korea Environmental Institute. Mongolian Nature and Environment Consortium. 2006.
- Lewin J, Macklin MG.: Metal mining and floodplain sedimentation in Britain. In: Gardiner V, editor. *International Geomorphology*. Wiley, Part 1, 1009–27, 1987.
- Lewis, W.M. and Grant, M.C.: Relationship between stream discharge and yield of dissolved substances from a Colorado mountain watershed. *Soil Science*, 128, 353-363, 1979.
- Lund, T.J. et al., 2008. Surface complexation modeling of Cu(II) adsorption on mixtures of hydrous ferric oxide and kaolinite, *Geochem T.*, 9(1), 9, 2008.
- Lychagin M.Yu., Tkachenko A.N., Kasimov N.S. and Kroonenberg S.B. Heavy Metals in the Water, Plants, and Bottom Sediments of the Volga River Mouth Area. *Journal of Coastal Research*. Published Pre-print online. 2013. (<http://dx.doi.org/10.2112/JCOASTRES-D-12-00194.1>)

- Macklin M.G., P.A. Brewer, K.A. Hudson-Edwards, G. Bird, T.J. Coulthard, I.A. Dennis, P.J. Lechler, J.R. Miller, J.N. and Turner., A.: geomorphological approach to the management of rivers contaminated by metal mining, *Geomorphology*, 79, 423–447, 2006.
- Malmström, M.E., Berglund, S., and Jarsjö, J.: Combined effects of spatially variable flow and mineralogy on the attenuation of acid mine drainage in groundwater, *Appl Geochem.*, 23, 1419-1436, 2008.
- MCA.: Midterm Report, Annex 4. Chapter 5.3 Water Quality. <http://en.mca.mn/file/545.shtml>. Accessed 14 April 2011, 2011.
- Mighanetara, K., Braungardt, C.B., Rieuwerts, J.S., and Azizi, F.: Contaminant fluxes from point and diffuse sources from abandoned mines in the River Tamar catchment, UK, *J Geochem Explor.*, 100, 116–124, 2009.
- Moldovan, B.J., and Hendry, J.M.: Characterizing and Quantifying Controls on Arsenic Solubility over a pH Range of 1–11 in a Uranium Mill-Scale Experiment, *Environ Sci and Tech.*, 39 (13), 4913-4920, 2005.
- Mukiibi, M., Ela, W.P. and Sáes, A.E.: Effect of ferrous iron on arsenate sorption to amorphous ferric hydroxide. *Ann N Y Acad Sci*, 1140, 335-345, 2008.
- Nystrand, M.I., Österholm, P., Nyberg, M.E., and Gustafsson, J.P.: Metal speciation in rivers affected by enhanced soil erosion and acidity, *Appl Geochem.*, 27, 906–916, 2012.
- Palleiro, L., Rodríguez-Blanco, M.L., Taboada-Castro, M.M., and Taboada-Castro, M.T.: The Influence of Discharge, pH, Dissolved Organic Carbon, and Suspended Solids on the Variability of Concentration and Partitioning of Metals in a Rural Catchment, *Water Air Soil Pollut.*, 224, 1–11, 2013.
- Persson, K., Jarsjö, J., and Destouni, G.: Diffuse hydrological mass transport through catchments: scenario analysis of coupled physical and biogeochemical uncertainty effects. *Hydrol Earth Syst Sci*, 15: 3195-3206. doi:10.5194/hess-15-3195-2011, 2011.
- Parkhurst, D.L. and Appelo, C.A.J.: User's guide to PHREEQC (Version 2)3195-2011,r program for speciation, batch reaction, one-dimensional transport, and inverse geochemical calculations. U.S. Geological Survey Water-Resources Investigations Report 99-4259, 312 pp, 1999.
- Pfeiffer, M., Batbayar, G., Hofmann, J., Siegfried, K., Karthe, D., and Hahn-Tomer, S.: Investigating arsenic (As) occurrence and sources in ground, surface, waste and drinking water in northern Mongolia, *Environ Earth Sci.*, DOI 10.1007/s12665-013-3029-0, 2014 (in Press).
- Pietron, J.: Modeling sediment transport in the downstream Tuul River, Mongolia, MSc thesis, INK, Stockholm University, 2012.
- Raguž, V., Jarsjö, J., Grolander, S., Lindborg, R., and Avila, R.: Plant uptake of elements in soil and pore water: Field observations versus model assumptions, *J Environ Manage.*, 126, 147-156, 2013.
- Raymond, P.A. and Saiers, J.E.: Event controlled DOC export from forested watersheds, *Biogeochemistry*, 100(1-3), 197–209, 2010.
- Rudneva, N.A., Pronin, N.M., and Rudneva, L.V.: Microelements and Metals in the Muscles of the Muskrat (*Ondatra zibethica*) from the Selenga River Delta, *Russ J Ecol.*, 36, 435–437, 2005.

- Sanches-España, J.S., Pamo, E.L., Pastor, E.S., Andrés, J.R., and Rubí J.A.M.: The Impact of Acid Mine Drainage on the Water Quality of the Odiel River (Huelva, Spain): Evolution of Precipitate Mineralogy and Aqueous Geochemistry Along the Concepción-Tintillo Segment, *Water Air Soil Poll.*, 173, 121–149, 2006.
- Saria, L., Shimaoka, T. and Miyawaki, K.: Leaching of heavy metals in acid mine drainage, *Waste Manag Res*, 24, 134140, 2006.
- Sauvé, S., Hendershot, W., and Allen, H.E.: Solid-Solution Partitioning of Metals in Contaminated Soils: Dependence on pH, Total Metal Burden, and Organic Matter, *Environ Sci Tech.*, 34, 1125–1131, 2000.
- Schelker, J., Eklöf, K., Bishop, K., and Laudon, H.: Effects of forestry operations on dissolved organic carbon concentrations and export in boreal first-order streams, *J. Geophys. Res.*, 117, G01011, doi:10.1029/2011JG001827, 2012.
- Scultz, M.F., Benjamin, M.M., and Ferguson, J.: Adsorption and Desorption of Metals on Ferrihydrite: Reversibility of the Reaction and Sorption Properties of the Regenerated Solid, *Environ Sci Tech.*, 21, 863-869, 1987.
- Sjöblom, Å., Håkansson, K., and Allard, B.: River Water Metal Speciation in a Mining Region – The Influence of Wetlands, Liming, Tributaries, and Groundwater, *Water Air Soil Poll.*, 152(1-4), 173–194, 2004.
- Sjöstedt, C., Wällstedt, T., Gustafsson, J.P., and Borg, H.: Speciation of aluminium, arsenic and molybdenum in excessively limed lake, *Sci Tot Environ.*, 407(18), 5119–5127, 2009.
- Sjöstedt, C.S., Gustafsson, J.P., and Köhler, S.J.: Chemical Equilibrium Modeling of Organic Acids, pH, Aluminum, and Iron in Swedish Surface Waters, *Environ Sci Tech.*, 44, 8587–8593, 2010.
- Sjöstedt, C., Persson, I., Hesterberg, D., Kleja, D.B., Borg, H., Gustafsson, J.P., 2013. Iron speciation in soft-water lakes and soils as determined by EXAFS spectroscopy and geochemical modelling. *Geochim Cosmochim Acta* 105, 172-186.
- Smedley, P.L., and Kinniburgh, D.G.: A review of the source, behaviour and distribution of arsenic in natural waters, *Appl Geochem.*, 17(5), 517–568, 2002. Smith, K.S.: Metal Sorption On Mineral Surfaces: An Overview With Examples Relating To Mineral Deposits, *Reviews in Economic Geology*, ch. 7, *The Environmental Geochemistry of Mineral Deposits*, 1999. Streat, M., Hellgardt, K., and Newton, N.L.R.: Hydrous ferric oxide as an adsorbent in water treatment: Part 2. Adsorption studies, *Process Saf Environ.*, 86, 11–20, 2008.
- Smith, R., Martell, A., Motekaitis, R., 2003. NIST Critically Selected Stability Constants of Metal Complexes Database. Version 7.0. NIST Standard Reference Database 46. National Institute of Standards and Technology, US Department of Commerce, Gaithersburg.
- Stumm, W., and Morgan, J.J.: *Aquatic Chemistry*. John Wiley & Sons. 1996.
- Tack, F.M.G., and Verloo, M.G.: Chemical Speciation and Fractionation in Soil and Sediment Heavy Metal Analysis: A Review, *Int J Environ An Ch.*, 59(2-4), 225–238, 1995.

- Tarras-Wahlberg, N.H., Flachier, A., Fredriksson, G., Lane, S., Lundberg, B., and Sangfors, O.: Environmental management of small-scale and artisanal mining: the Portovelo-Zaruma goldmining area, southern Ecuador, *J Environ Manage*, 65, 165–179, 2000.
- Tessier, A., and Campbell, P.G.C.: Partitioning of trace metals in sediments: Relationships with bioavailability, *Hydrobiologia*, 149(1), 43–52, 1987.
- Thorslund, J., Jarsjö, J., Chalov, S.R., and Belozeroва, E.V.: Gold mining impact on riverine heavy metal transport in a sparsely monitored region: the upper Lake Baikal Basin case, *J Environ Monit.*, 14, 2780–2792, 2012.
- Tiberg, C., Sjöstedt, C., Persson, I., and Gustafsson, J.P.: Phosphate effects on copper(II) and lead(II) sorption to Ferrihydrite, *Geochim Cosmochim Acta.*, 120, 140–157, 2013.
- Tipping, E.: WHAMC - a chemical equilibrium model and computer code for waters, sediments, and soils incorporating a discrete site/electrostatic model of ion-binding by humic substances, *Comput. Geosci.*, 20, 973–1023, 1994.
- Tipping, E., Lofts, S., and Lawlor, A.: Modeling the chemical speciation of trace metals in the surface waters of the Humber system, *Sci Tot Environ.*, 210, 63–77, 1998.
- Tipping E., Rey-Castro C., Bryan S. E., and Hamilton-Taylor J. (2002) Al(III) and Fe(III) binding substances in freshwaters, and implications for trace metal speciation. *Geochim. Chosmochim. Acta*, 66, 3211-3224.
- Törnqvist, R., Jarsjö, J., and Karimov, B.: Health risks from large-scale water pollution: Trends in Central Asia. *Environ Int*, 37, 435-442, 2011.
- USGS.: Lake Baikal's Selenga River Delta: Biodiversity, Conservation and Sustainable Development. Institute of General and Experimental Biology, Siberian Branch, Russian Academy of Sciences, Ulan-Ude, Russia. <http://deltas.usgs.gov/rivers.aspx?river=selenga>. Accessed latest October 22, 2013. 2011.
- van Geen, A., Adkins, J.F., Boyle, E.A., Nelson, C.H., Palanques, A.: A 120-yr record of widespread contamination from mining of the Iberian pyrite belt. *Geology* 25, 291–294, 1997.
- Weng, L., Temminghoff, E.J.M., Lofts, S., Tipping, E., and Van Riemsdijk, W.H.: Complexation with Dissolved Organic Matter and Solubility Control of Metals in a Sandy Soil, *Environ. Sci. Technol.*, 36, 4804–4810, 2002.
- Weerasooriya, R., Aluthpatabendi, D., and Tobschall, H.J.: Charge distribution multi-site complexation (CD-MUSIC) modeling of Pb(II) adsorption on gibbsite, *Colloids and Surfaces A: Physicochemical and Engineering Aspects*, 189, 131-144, 2001.
- WHO.: Guidelines for drinking water Quality. Vol. 1, 3rd ed. World Health Organization. Geneva. 2006.
- Wällstedt, T., Björkvald, L., and Gustafsson, J.P.: Increasing concentrations of arsenic and vanadium in (southern) Swedish streams, *Appl Geochem.*, 25, 1162–1175, 2010.
- Yoshioka, T., Ueda, S., Khodzher, T., Bashenkhaeva, N., Korovyakova, I., Sorokovikova, L., and Gorbunova, L.: Distribution of dissolved organic carbon in Lake Baikal and its watershed, *Limnology*, 3(3), 0159–0168,

2002.Zandaryaa, S., Aureli, A., Merla, A., and Janchivdorj, L.: Transboundary Water Pollution in Baikal Lake Basin: The Role of Surface-Ground water Interactions and Groundwater. In : Basandorj,D. and Oyunbaatar, D. (eds), International conference “Uncertainties in Water Resource Management: causes, technologies and consequences” . IHP Technical Documents in Hydrology, 1, 94-105, 2008.

Zhao, G., Wu, X., Tan, X., and Wang, X.: Sorption of Heavy Metal Ions from Aqueous Solutions: A Review, The Open Colloid Science Journal, 2011, 19-31, 2011.

## Tables

**Table 1. Sampling information (locations, names and dates) of the water samples collected in the Tuul and Sharyngol rivers and the surface water ponds in 2012 and 2013.**

<i>Sample</i>	<i>Date</i>	<i>Location</i>	<i>Longitude</i>	<i>Latitude</i>
			<i>(decimal degrees)</i>	
<b>T2</b>	2013-09-08	Tuul River, Ulaanbaatar	107.056	47.973
<b>T3</b>	2013-09-08	Tuul River, downstream Ulaanbaatar	106.767	47.957
<b>T4</b>	2013-09-09	Tuul River, downstream Ulaanbaatar	105.198	47.862
<b>T5</b>	2012-06-24 2013-09-14	Tuul River, upstream of Zaamar site	104.523	48.014
<b>T5a</b>	2012-06-24 2013-09-14	Tuul River, start of Zaamar site	104.306	48.158
<b>T5b</b>	2012-06-23 2013-09-12	Tuul River, at Zaamar site	104.325	48.229
<b>T6</b>	2012-06-23 2013-09-11	Tuul River, at Zaamar site	104.420	48.332
<b>T6a</b>	2012-06-23 2013-09-11	Tuul River, downstream of Zaamar site	104.512	48.389
<b>T6b</b>	2013-09-11	Tuul River, downstream of Zaamar site	104.652	48.675
<b>T7</b>	2013-09-13	Tuul River, just before conjunction with Orkhon River	104.798	48.948
<b>S1</b>	2013-09-13	Sherengol River, upstream mining area	102.845	49.379
<b>S2</b>	2013-09-13	Sherengol River, downstream mining area	106.403	49.239

<i>S3</i>	2013-09-13	Sherengol River, downstream mining area	106.270	41.410
<i>S5</i>	2013-09-13	Sherengol River, downstream mining area		
<i>P1</i>	2013-09-12	Pond at Zaamar site	104.230	48.179
<i>P3</i>	2013-09-11	Pond at Zaamar site	104.302	48.189
<i>P4</i>	2013-09-11	Pond at Zaamar site	104.304	48.190

Table 2. Selected oxidation states of the various components for the input file in Visual Minteq. Because samples were collected from river water, well-oxygenated conditions were assumed, and thus oxidised forms of the elements were chosen.

Al<sup>3+</sup>, As (V), Ca<sup>2+</sup>, Cd<sup>2+</sup>, Co<sup>2+</sup>, Cr(VI), Cu<sup>2+</sup>, Fe<sup>3+</sup>, K<sup>1+</sup>, Mg<sup>2+</sup>, Mn<sup>2+</sup>, Mo(VI), Na<sup>1+</sup>, Ni<sup>2+</sup>, P (PO<sub>4</sub>), Pb<sup>2+</sup>, S (SO<sub>4</sub>), Cl<sup>-1</sup>, Si (H<sub>4</sub>SiO<sub>4</sub>), V(V), Zn<sup>2+</sup>

Table 3. Reactions and reaction constants of the possible solid phases allowed to precipitate if their solubility constant (log Ks) is exceeded (equations from Visual Minteq).

<i>Mineral</i>	<i>Reaction</i>	<i>Log Ks (25°C)</i>
Aluminium hydroxide (soil)	Al(OH) <sub>3</sub> + 3H <sup>+</sup> = Al <sup>3+</sup> + 3H <sub>2</sub> O	8.29
Calcite	CaCO <sub>3</sub> + 2H <sup>+</sup> = Ca <sup>2+</sup> + CO <sub>2</sub> (g) + H <sub>2</sub> O	-8.48
Ferrihydrite (aged)	Fe(OH) <sub>3</sub> + 3H <sup>+</sup> = Fe <sup>3+</sup> + 3H <sub>2</sub> O	2.69
Gibbsite (C)	Al(OH) <sub>3</sub> + 3H <sup>+</sup> = Al <sup>3+</sup> + 3H <sub>2</sub> O	7.74
Manganite	MnOOH + 3H <sup>+</sup> = Mn <sup>3+</sup> + 2H <sub>2</sub> O	25.3

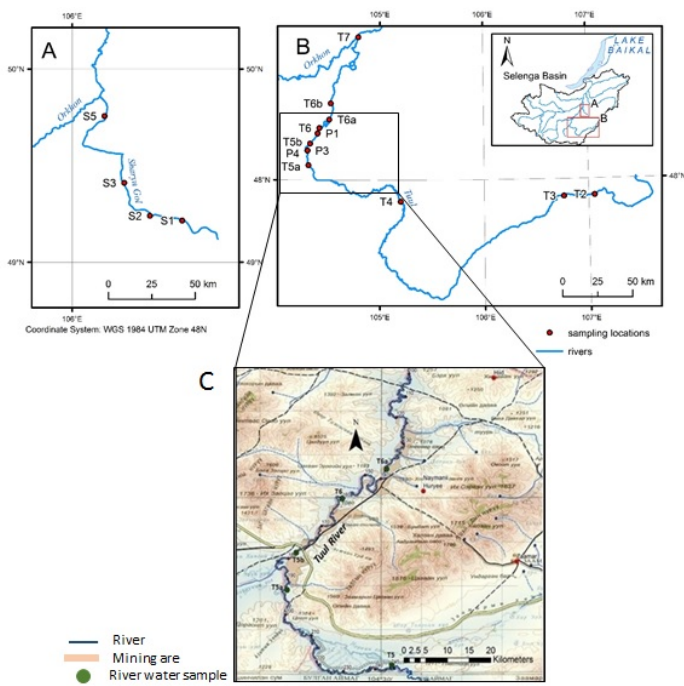
Table 4. Measured geochemical parameters in all sample locations from 2012 and 2013. a) calculated according to Equation (4).

<i>Parameter/ Site</i>	<i>pH</i>	<i>Temp (°C)</i>	<i>Pe<sup>a</sup></i>	<i>Alkalinity (meq/l)</i>	<i>DOC (mg/l)</i>
	2012/2013	2012/2013	2012/2013	2012/2013	2013
<i>T2</i>	6.7 (2013)	12.1 (2013)	13.6 (2013)	8.5 (2013)	9.0



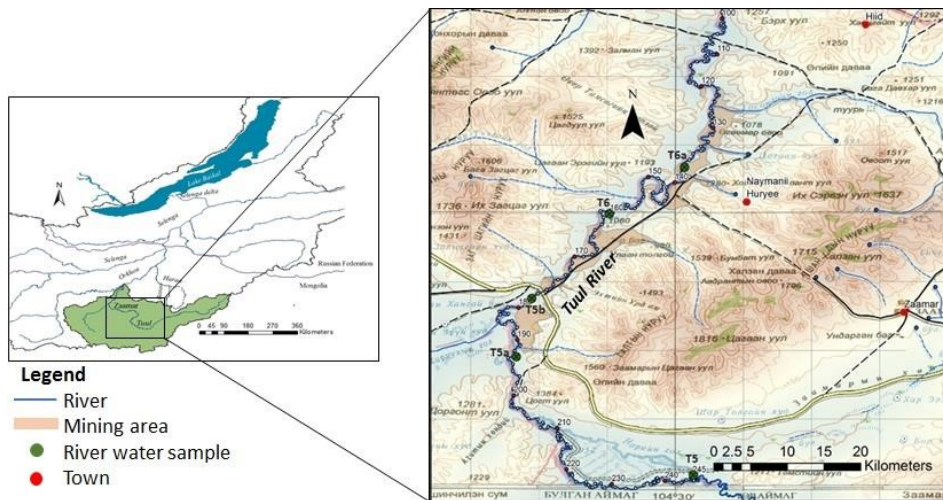
<b>T3</b>	7.1 (2013)	13.4 (2013)	13.4 (2013)	6.8 (2013)	8.3
<b>T4</b>	8.0 (2013)	13.5 (2013)	13.5 (2013)	5.1 (2013)	9.0
<b>T5</b>	9.2/9.2	16.9/19.5	11.9/12.1	2.1/8.5	11.7
<b>T5a</b>	9.6/7.6	19.2/17.0	11.0/13.0	1.6/8.5	11.2
<b>T5b</b>	8.8/8.0	22.4/17.0	11.8/12.6	1.6/5.1	10.7
<b>T6</b>	8.5/8.8	19.1/17.0	12.1/11.8	1.5 <sup>c</sup> /5.1	11.5
<b>T6a</b>	8.7/8.5	19.1/15.6	12.3/12.1	1.3 <sup>b</sup> /5.1	11.7
<b>T6b</b>	8.1 (2013)	15.0 (2013)	12.5 (2013)	8.5 (2013)	11.8
<b>T7</b>	8.2 (2013)	18.9 (2013)	12.4 (2013)	8.5 (2013)	9.4
<b>S1</b>	8.2 (2013)	9.9 (2013)	12.4 (2013)	1.6 (2013)	10.8
<b>S2</b>	8.3 (2013)	9.4 (2013)	12.3 (2013)	1.6 (2013)	10.7
<b>S3</b>	8.1 (2013)	10.4 (2013)	12.5 (2013)	1.6 (2013)	10.7
<b>S5</b>	8.2 (2013)	9.9 (2013)	12.4 (2013)	1.6 (2013)	10.7
<b>P1</b>	8.7 (2013)	12.0 (2013)	11.9 (2013)	1.6 (2013)	7.0
<b>P3</b>	8.7 (2013)	12.0 (2013)	11.9 (2013)	1.6 (2013)	11.0
<b>P4</b>	8.7 (2013)	12.0 (2013)	11.9 (2013)	1.6 (2013)	10.7

## Figures

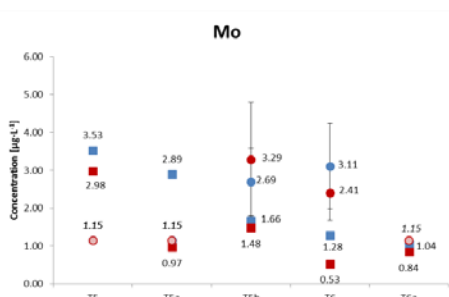
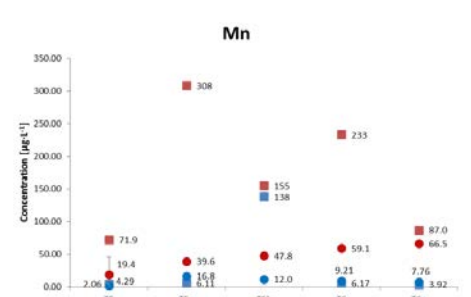
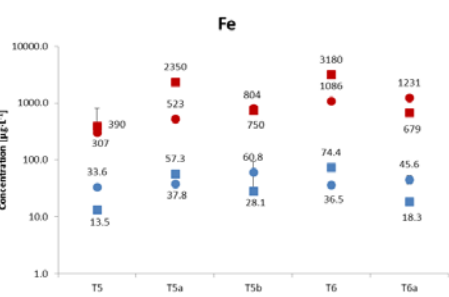
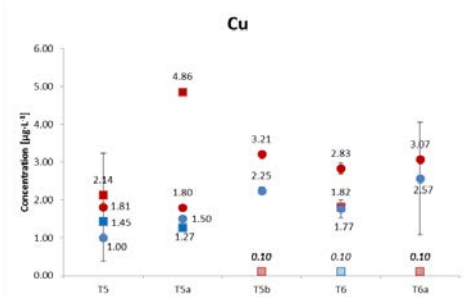
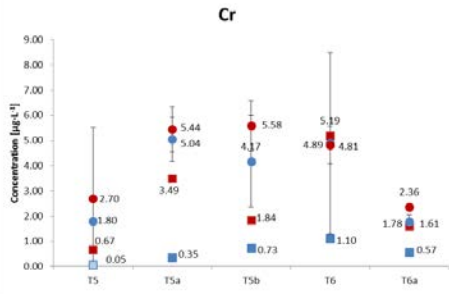
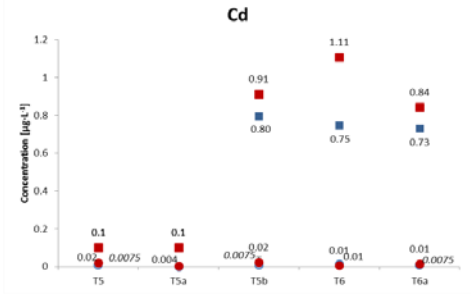
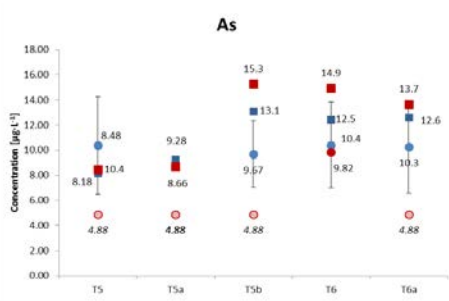
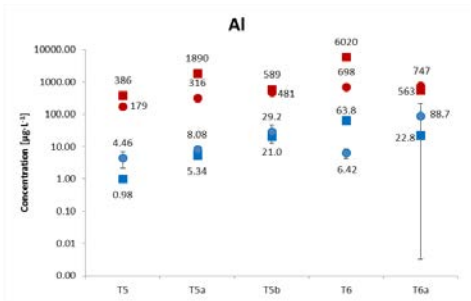


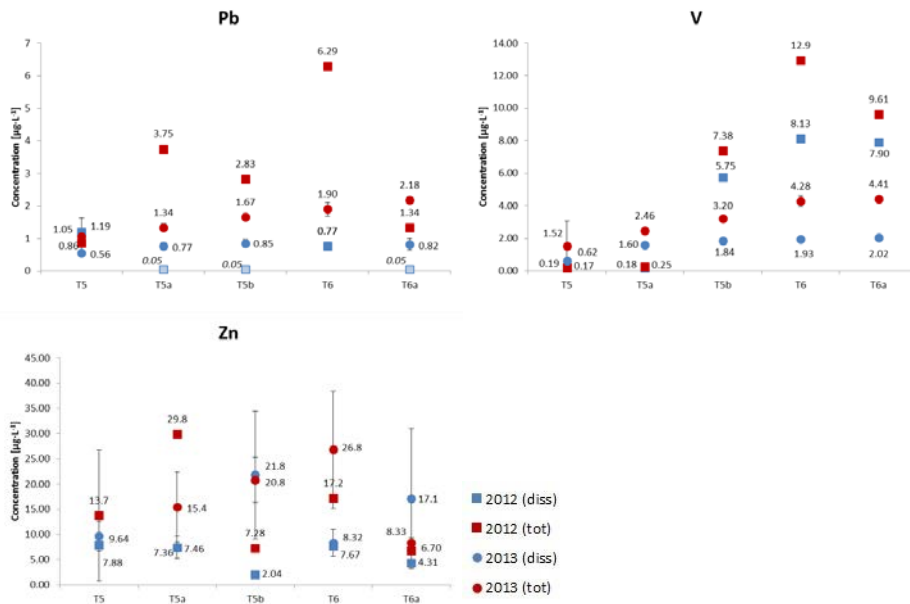
Formatted: Keep with next

**Figure 1. Map showing the two sampled rivers; Tuul River (A) and Sharvngol River (B) within the Lake Baikal Basin. A zoomed map with the Zaamar mining area located along the Tuul River where ponds were sampled and where mining areas are marked is shown in C. (Author: J. Pietron).**

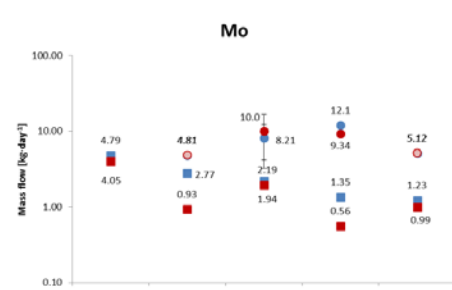
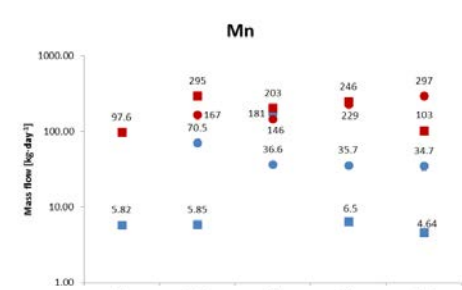
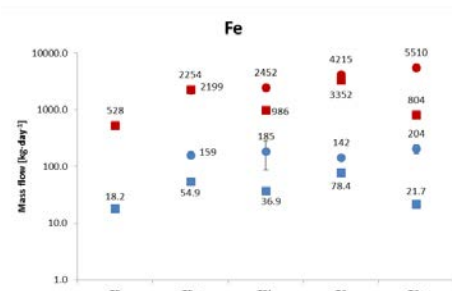
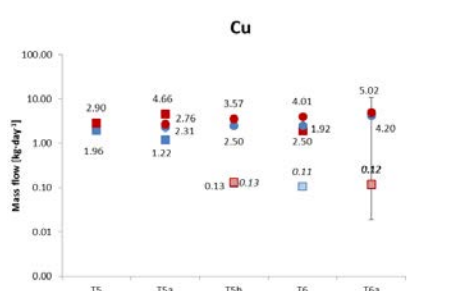
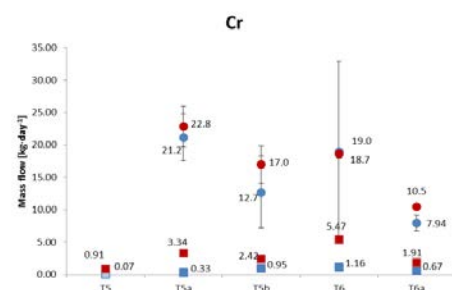
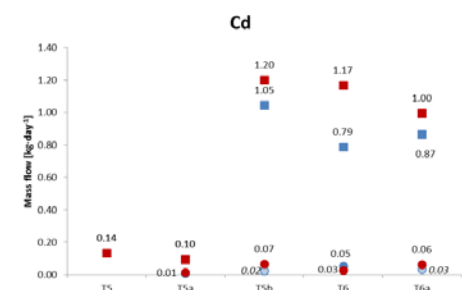
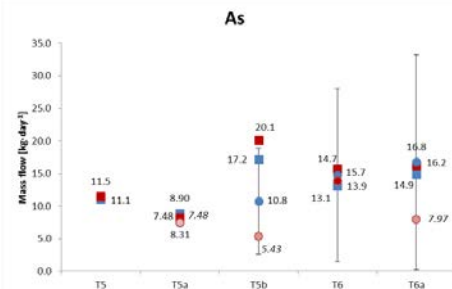
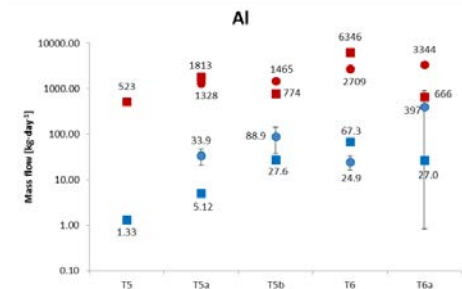


**Figure 1.** Map of the Baikal Basin with the Zaamar mining area (zoomed) located in the Mongolian part of the basin along the Tuul River (Author: J. Thorslund).





**Figure 2.** Dissolved (blue) and total (red) concentrations of Al, As, Cd, Cr, Cu, Fe, Mn, Mo, Pb, V and Zn at the five sampling locations along the Tuul River focus reach and the Zaamar Goldfield from the sampling campaigns in 2012 (squares) and 2013 (circles). In the case of no detectable results, the midpoint of the possible concentration range is shown in a lighter colour for illustrative purposes (see SI for DL values).



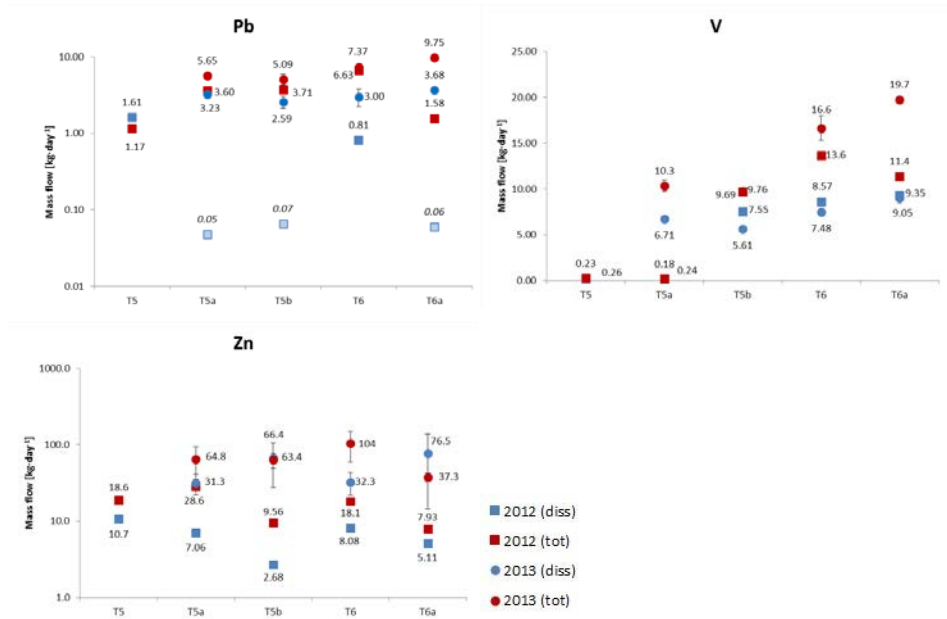
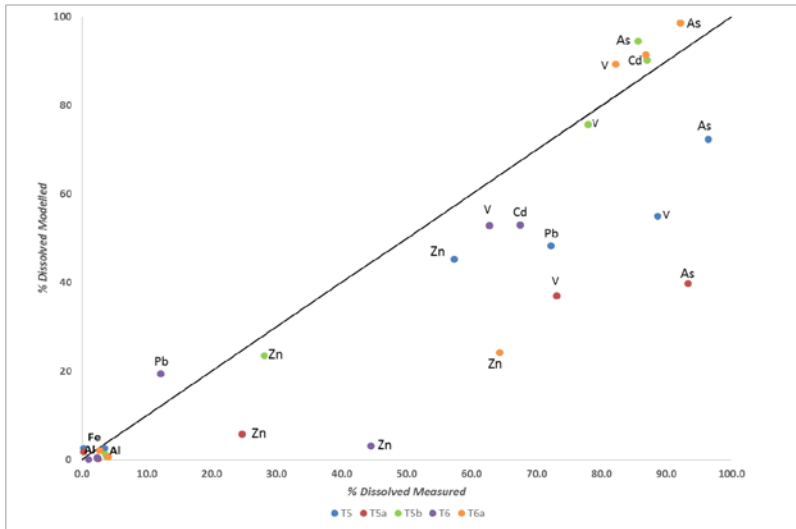


**Figure 3.** Estimated dissolved (blue) and total (red) mass flows, in kg per day, of Al, As, Cd, Cr, Cu, Fe, Mn, Mo, Pb, V and Zn at the five sampling locations (T5-T6a) along the Tuul River focus reach and the Zaamar Goldfield from the sampling campaigns in 2012 (squares) and 2013 (circles).

(a)



(b)

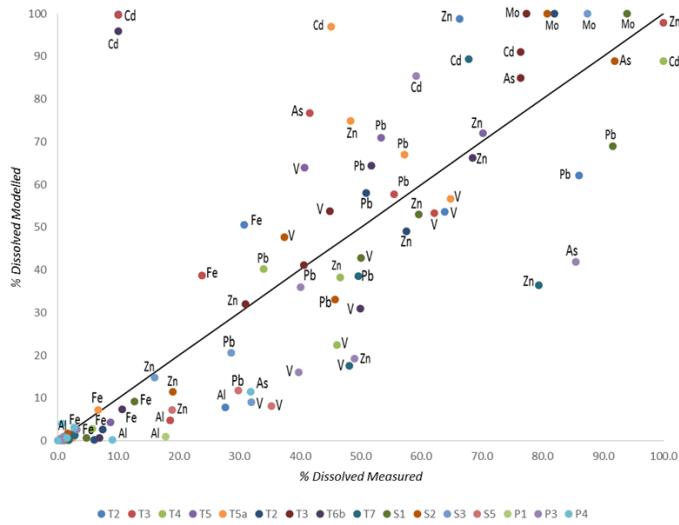


**Figure 4.** Comparison between measured and modelled results for the dissolved fractions (percentage) of metals in the (a) 2012 campaign and the (b) 2013 campaign.



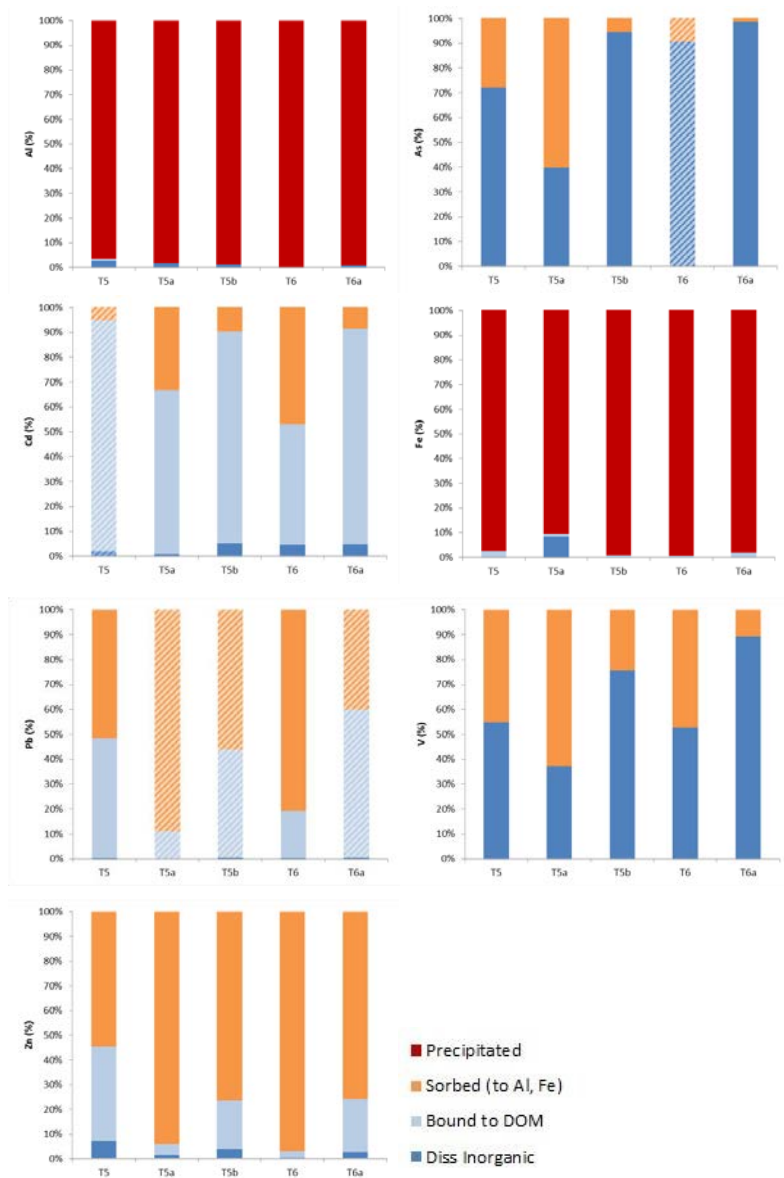


**Figure 5.** Predicted speciation of the selected metals ('dissolved inorganic', 'bound to DOM', 'sorbed' or 'precipitated') for the five sampling locations along the Tuul River in the 2012 campaign.

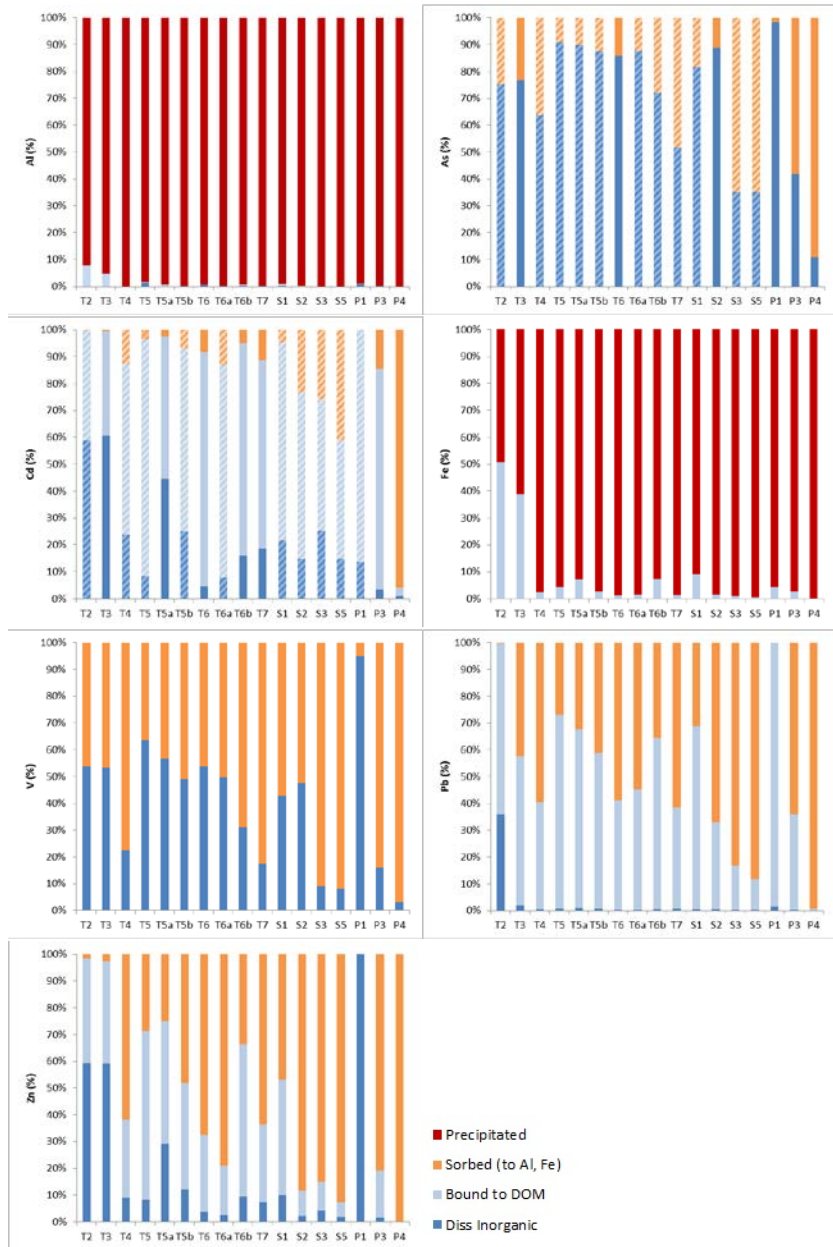


**Figure 6.** Predicted speciation of the selected metals ('dissolved inorganic', 'bound to DOM', 'sorbed' or 'precipitated') in the five sampling locations along the Tuul River in the 2013 campaign.

